

Frequency Control of Power System with Distributed Sources by Adaptive Type 2 Fuzzy PID Controller

Srinivasan Kullapadayachi Govindaraju, Raghuraman Sivalingam, Sidhartha Panda, Preeti Ranjan Sahu & Sanjeevikumar Padmanaban

To cite this article: Srinivasan Kullapadayachi Govindaraju, Raghuraman Sivalingam, Sidhartha Panda, Preeti Ranjan Sahu & Sanjeevikumar Padmanaban (2023): Frequency Control of Power System with Distributed Sources by Adaptive Type 2 Fuzzy PID Controller, Electric Power Components and Systems, DOI: [10.1080/15325008.2023.2227169](https://doi.org/10.1080/15325008.2023.2227169)

To link to this article: <https://doi.org/10.1080/15325008.2023.2227169>



Published online: 29 Jun 2023.



Submit your article to this journal [↗](#)




View related articles [↗](#)



View Crossmark data [↗](#)



Frequency Control of Power System with Distributed Sources by Adaptive Type 2 Fuzzy PID Controller

Srinivasan Kullapadayachi Govindaraju,¹ Raghuraman Sivalingam,² Sidhartha Panda,³ Preeti Ranjan Sahu,⁴ and Sanjeevikumar Padmanaban ⁵

¹Department of Electrical and Electronics Engineering, Mahendra Engineering College for women, Namakkal, Tamil Nadu, India

²Department of Electrical and Electronics Engineering, Velammal Engineering College, Surapet, Chennai, Tamil Nadu, India

³Department of Electrical and Electronics Engineering, Veer Surendra Sai University of Technology, Burla, Odisha, India

⁴Department of Electrical and Electronics Engineering, NIST Institute of Science & Technology, Berhampur, Odisha, India

⁵Department of Electrical Engineering, IT and Cybernetics, University of South-Eastern Norway, Porsgrunn, Norway

CONTENTS

1. Introduction
 2. Investigation of Hybrid Power System
 3. Adaptive Type 2 Fuzzy PID Structure
 4. Optimization Problem
 5. Sine Cosine Adopted Improved Equilibrium Optimization (SCaIEO) Algorithm
 6. Results and Discussion
 7. Conclusion
- References

Abstract—The unpredictability of solar and wind energy sources affects contemporary power networks and adds frequency variations. An appropriate intelligent controller is necessary to balance electricity between generation and demand. As a result, in this research, we present a sine-cosine adaptive improved equilibrium optimization (SCaIEO) method tuned to Adaptive Type 2 Fuzzy PID Controller (AT2FPID) for frequency management of cutting-edge power systems. The efficiency of the SCaIEO approach is assessed by comparing it to the original equilibrium optimization (EO) and other comparable algorithms for the test function. Moreover, engineering applications of the SCaIEO technique are carried out by constructing an AT2FPID controller to manage the frequency of power systems that include renewable energy and dispersed sources. First, we show that SCaIEO outperforms EO, Particle Swarm Optimization, Genetic Algorithm, Moth Flame Optimization, and Gravitational Search Algorithm in the PID controller (Gravity Search Algorithm). The AT2FPID is next evaluated, and the SCaIEO AT2FPID controller's dominance is proven by equating the outcome to the original, PID Type 1 Fuzzy PID, Type 2 Fuzzy PID controller.

Keywords: improved equilibrium optimization, sine cosine adopted improved equilibrium optimization, distributed power generation, adaptive control

Received 2 March 2023; accepted 11 June 2023

Address correspondence to Preeti Ranjan Sahu, Department of Electrical and Electronics Engineering, NIST Institute of Science & Technology, Berhampur 761008, Odisha, India. E-mail: preetiranjan.sahu@nist.edu

1. INTRODUCTION

Renewable energy networking decreases dependency on non-renewable resources, which causes generation load disparity and frequency variations. The frequency variation is kept within an acceptable range by the load frequency controller (LFC) [1]. According to a survey of the literature, numerous approaches have been devised to handle the load frequency problem [2–5]. In traditional power systems (PS), most techniques to LFC are focused on frequency

control. Few studies, however, have looked at the influence of renewable and decentralized energy sources in the LFC context. As a result, we suggest an LFC technique in this study in which renewable and decentralized resources exist in the traditional energy system.

In the past, studies have shown that managing a PS's operating frequency relies on the controller setup and the method used to derive controller parameters. Conventional PID-based techniques may not deliver the desired performance for complex systems [6–8]. In contrast, FLC (Fuzzy Logic Controller) may increase PID controller performance and deal with non-linearity and uncertainty. An FLC-based controller's design comprises the right selection of scaling factors (SF) for inputs and/or outputs, as well as other parameters. There are several FLC-based controllers available, such as hybrid particle swarm optimization (PSO)-PS regulated FLC [6], ICA tuned to fractionally ordered (FO) fuzzy logic-based PID (FPID) [7], and BFOA pitched to FO FPID [8]. With big uncertainty, conventional fuzzy controllers may be inefficient. In this scenario, however, the second type of FPID structure (T2FPID) based on the twin membership function gives enhanced dynamics [9]. The T2FPID setup can be altered to correspond to the recommendations for fuzzy PID controllers [10]. In this research, we present an adaptive T2FPID controller (AT2FPID), which takes an input signal and applies it to the fuzzy type 2 and PID controllers, changing the output control operation correspondingly.

In accordance with an investigation into the literature, numerous strategies are used to build AGC controllers. In Ref. [11], a Simple Grey Wolf Optimizer (SGWO) scheme was presented for an Adaptive Fuzzy PID (AFPID) structure for a power system with energy storage through EV. In Ref. [12], a three-dimensional fuzzy-PID structure is proposed to regulate the frequency of a different energy integrated power system. [13] Proposes a resilient fractional ordered 3DOF-FOPID structure for frequency control in a distributed power system. [14] Presents a hybrid technique for electric power system frequency management. [15] Investigates a 2DOF-PIDN-FOID frequency control scheme. Other strategies, such as the “Grasshopper optimization algorithm (GOA),” are also used. “Sunflower optimization (SFO),” [16] “Sine Cosine Algorithm (SCA),” [17] “PSO” [18], and “Search for symbiotic organisms (SOS)” [19], the Equilibrium Optimization (EO) Algorithm [20, 21].

Design of a PID regulator using Kharitonov theorem and future search algorithm for an Automatic Voltage Regulator (AVR) is presented in Ref. [22]. The results are

compared with Teaching–Learning–Based Optimization (TLBO), Artificial Bee Colony (ABC), non-dominated sorting genetic algorithm (GA) II, and multi-objective extremal optimization to demonstrate the superiority. In Ref. [23], the charging scheme of batteries is achieved by employing a hybrid GA tuned PI controller with adaptive neuro-fuzzy inference system in a isolated PS with wind & solar energies and batteries for load management. Fuzzy logic (FL) and Harris Hawks optimization-based energy management system is proposed for a seawater desalination plant to attain the best performance under variations and uncertainty in energy price has been presented in Ref. [24]. An imperialist competitive algorithm tuned neural network predictive controller for automatic voltage regulator is proposed in Ref. [25]. The results are equated with GA-tuned NN and Ziegler–Nichols-based PID controller to authenticate the advantage. Frequency control of a three-area hybrid PS using honey badger algorithm-based FOPID controller has been proposed in Ref. [26]. It is demonstrated that the proposed approach is suitable for the frequency regulation with different RES penetration and under parameter variation. A modified multiverse optimizer method to tune the values of a 2 degree of freedom fuzzy PID structure for LFC of microgrid (MG) systems has been presented in Ref. [27]. The superiority of MMVO technique over MVO, GWO, gravitational search algorithm, GA and PSO has been shown using benchmark test functions. Marine predator algorithm tuned PD-(1 + PI) structure LFC of MG system is proposed in Ref. [28]. To exhibit its dominance, the algorithm is equated with GA, Differential Evolution (DE), and Grey Wolf Optimization (GWO) techniques. A modified EO scheme using scaling factors is proposed in Ref. [29] for LFC of interconnected distributed PS. The scheme is equated with EO and similar techniques in benchmark test functions. A detailed study of recent progress in the meta-heuristics field is presented in Ref. [30].

It is observed from literature survey that innovative strategies for solving optimization issues are constantly welcome. Equilibrium Optimizer (EO) has recently been designed to address optimization challenges [31]. Although the EO technique is effective, it has a few drawbacks [32]. The biggest issue with EO is that it might become caught in local minima [33]. As a result, in this study, the EO technique is improved by using Sine Cosine adopted scaling factors to control the progress of parameters during iterations in the EO algorithm. The use of Scaling Factors (SFS) using Sine and Cosine expressions improves the symmetry of the exploration and exploitation mix in the search method.

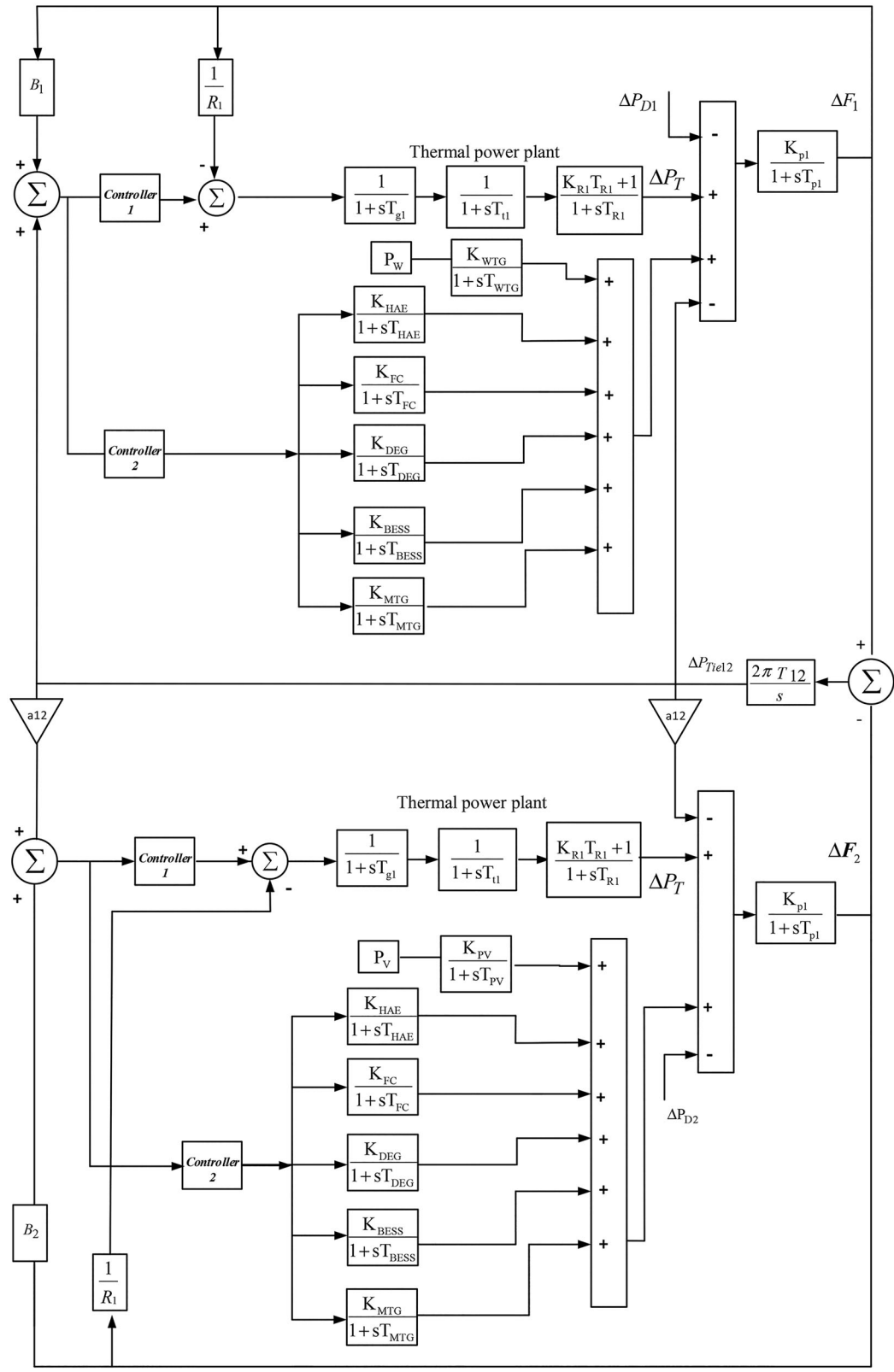


FIGURE 1. Hybrid multi-area system (a) T1FPID and T2FPID (b) AT2FPID.

Hence, in this work, the AT2FPID controller is tuned using the SCAEIO algorithm for LFC of the PS with dispersed and non-conventional sources. This work's contributions are:

- By incorporating Sine Cosine adopted SFS into the standard EO method, the Sine Cosine adopted improved EO (SCAIEO) approach is created.
- The SCAIEO method is compared to EO and other processes such as the ABC algorithm [34], GA [35], Cuckoo Search (CS) [36], PSO [37], GSA [38], Hybrid PSO and GSA (PSO-GSA) [39], Water Cycle Algorithm (WCA) [40], Moth Flame Optimization (MFO) [41], Dragonfly Algorithm (DA) [42], and hybrid WCA-MFO [43].
- To assess SCAIEO's effectiveness in engineering design problems using EO, GSA, MFO, PSO, and GA methodologies.
- Systems related to various controllers were explored in relation to SCAIEO-based AT2FPID for frequency management under various altered circumstances.

2. INVESTIGATION OF HYBRID POWER SYSTEM

Figure 1 depicts the investigated PS, which includes thermal unit distributed generation (DG) sources. Photovoltaics (PV), Hydro Aqua Electrolyzers (HAE), Wind Energy Generator (WEG), Battery Energy Storage System (BESS), Fuel cell (FC), Diesel Engine Generator (DEG), Micro Turbine (MTG), and other sources are included in the DG system [44, 45]. Table 1 lists the relevant parameters.

2.1. Modeling of Various Components in the Studied System

2.1.1. *Wind Energy Generator.* The WEG is characterized by its different parameters. The ratio of tip speed given by: [44]:

$$\lambda = \frac{R_{\text{blade}} \omega_{\text{blade}}}{V_W} \quad (1)$$

where R_{blade} is the blade radius and ω_{blade} is blade speed. The C_p is found as:

$$C_p = (0.44 - 0.0167\beta) \sin \left[\frac{\Pi(\lambda - 3)}{15 - 0.3\beta} \right] - 0.0184(\lambda - 3)\beta \quad (2)$$

The output power of WEG is:

$$P_{WP} = \frac{1}{2} \rho A_R C_P V_W^3$$

where ρ is density of atmospheric air and A_r is swept area of turbine blade.

Components	Gain (K)	Time constant (T)
Thermal power system	$B = 0.425, K_r = 0.5, K_P = 120$	$T_g = 0.08, T_t = 0.3, T_r = 10.0, T_{12} = 0.0866, T_P = 20.0$
Wind energy generator	$K_{WEG} = 1$	$T_{WEG} = 1.5$
Photovoltaic system	$K_{PV} = 1$	$T_{PV} = 1.8$
Micro-turbine	$K_{MTG} = 1$	$T_{MTG} = 1.5$
Fuel cell	$K_{FC} = 0.01$	$T_{FC} = 4$
Hydro-aqua electrolyzer	$K_{HAE} = 0.002$	$T_{HAE} = 0.5$
Diesel energy storage system	$K_{DEG} = 0.003$	$T_{DEG} = 2$
Flywheel energy storage system	$K_{FESS} = -0.01$	$T_{FESS} = -0.1$

TABLE 1. Parameters of the studied system.

\dot{e}					
e	EXN	LN	ZER	LP	EXP
EXN	EXN	EXN	LN	LN	ZER
LN	EXN	LN	EXN	ZER	LP
ZER	LN	LN	ZER	LP	LP
LP	LN	ZER	LP	LP	EXP
EXP	ZER	LP	LP	EXP	EXP

TABLE 2. Rule-base for 3MFs.

WEG is represented by a transfer function (TF) as [44]:

$$G_{WEG_k}(s) = \frac{K_{WEG}}{1 + sT_{WEG}} \quad (3)$$

2.1.2. *Solar PV Modeling.* The output power from solar photovoltaic given by [11]:

$$P_{pv} = \eta S \gamma [1 - 0.005(T + 25)], \quad (4)$$

where η = PV cell conversion efficiency taken as 10%, S = PV array area equal to 4084 m²

ϕ = solar irradiation in kW/m² and T_a = ambient temperature ($T = 25^\circ\text{C}$).

This system's transfer function is

$$G_{PV}(s) = \frac{K_{PV}}{1 + sT_{PV}} = \frac{\Delta P_{PV}}{\Delta \phi} \quad (5)$$

2.1.3. *Hydrogen Aqua-Electrolyzer.* The transfer function of HAE is [11]:

$$G_{HAE}(s) = \frac{K_{HAE}}{1 + sT_{HAE}} \quad (6)$$

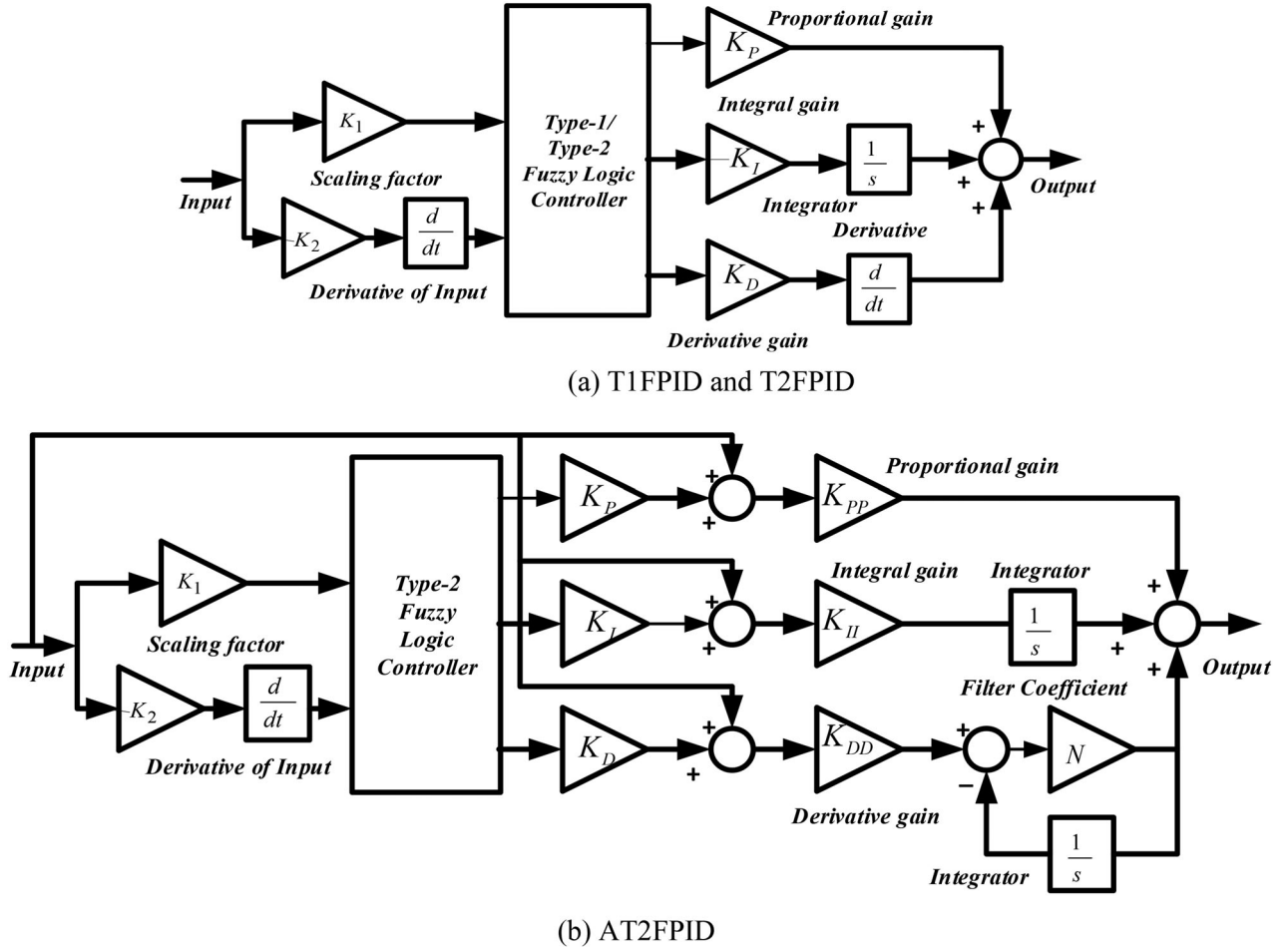


FIGURE 2. T1FPID, T2FPID, and AT2FPID controller structures.

2.1.4. *Fuel Cell.* The fuel cell's TF is [11]:

$$G_{FC}(s) = \frac{K_{FC}}{1 + sT_{FC}} \quad (7)$$

2.1.5. *Diesel Engine Generator.* The diesel energy generator's TF is:

$$G_{DEG}(s) = \frac{K_{DEG}}{1 + sT_{DEG}} \quad (8)$$

2.1.6. *Battery Energy Storage System.* The BESS has its rate constraints to deal with the electromechanical character and work in the non-linear zone and represented by [11]:

$$G_{BESS}(s) = \frac{K_{BESS}}{1 + sT_{BESS}} \quad (9)$$

2.1.7. *Micro-Turbine Generator.* The TF for a micro-turbine is [11]:

$$G_{MTG}(s) = \frac{K_{MTG}}{1 + sT_{MTG}} \quad (10)$$

2.1.8. *Thermal Control Unit.* The thermal control unit is made up of a turbine, re-heater and a governor with TFs [20]:

$$G_g(s) = \frac{K_g}{1 + sT_g} \quad (11)$$

$$G_t(s) = \frac{K_t}{1 + sT_t} \quad (12)$$

$$G_r(s) = \frac{1 + sK_rT_r}{1 + sT_r} \quad (13)$$

Equations (11)–(13) shows the transfer function model of governor, turbine and re-heater system, respectively.

2.1.9. Load. The TF of the load power system is [1]:

$$G_p(s) = \frac{K_P}{1 + sT_P} \quad (15)$$

3. ADAPTIVE TYPE 2 FUZZY PID STRUCTURE

3.1. Controller Structure

Given significant uncertainties, standard FLC may be ineffective for improving system performance. In this situation, the paired Membership function-based Type 2 (T2) controller performs enhanced. The structure proposed in this study is an adaptive type 2 fuzzy PID (AT2FPID), where the input signal is fed to T2 fuzzy PID. AT2FPID's efficacy is comparable to its previous generations. T1FPID/T2FPID structure is shown in Figure 2(a), while AT2FPID structure is shown in Figure 2(b). Upper (UMF) and lower (LMF) are employed as the MFs of the type 2 FLC (LMF) as shown in Figure 3. A barrier is formed when you combine UMF with LMF. A footprint of uncertainty (FOU) is created by constraining UMF and LMF.

Starting stage in fuzzy control is fuzzification where the input data are analyzed and needed fuzzy sets are created using MFs. The language words utilized for MFs include Extreme Negative (EXN), Least Negative (LN), Zero (ZER), Least Positive (LP), and Extreme Positive (EXP).

The type 2 fuzzy set is:

$$FS = ((Var, a), \mu_U(Var, a)), \nu Var \in P, \nu a \in J_{Var}[0, 1] \quad (16)$$

where $\mu_U(Var, a)$ is the UMF, Var is the main variable, a is the added variable of domain J_{Var}

The universe of discourse is expressed as:

$$FS = \int_{Var \in Pa \in J_{Var}[0,1]} \int \frac{\mu_E(Var, a)}{(Var, a)} \quad (17)$$

where \int = Union on ACE and a

$$\mu_U(Var, a) = \overline{FOU(U)} \nu Var \in P, \nu a \in J_{Var}[0, 1] \quad (18)$$

where J_{Var} is expressed as:

$$J_{Var} = [\mu_U(Var, a), \mu_L(Var, a)] \nu Var \in P, \nu a \in J_{Var}[0, 1] \quad (19)$$

The MF linked with type 1 FLC motivates to nurture LMF and UMF.

Table 2 shows the rule basis.

Individually Var and $dAVar$ are the inputs to type 2 Fuzzy logic controller which produces output y .

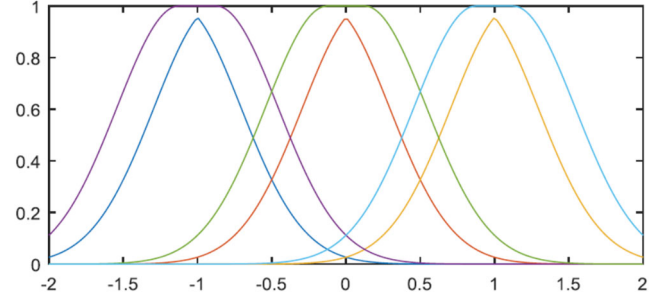


FIGURE 3. MFs of T2F controller.

The representative of the T2 FLC is

$$LMF : for Var = \underline{LN}; dVar = \underline{Z}; Y = \underline{LN} \quad (20)$$

$$UMF : for Var = \overline{LN}; dVar = \overline{Z}; Y = \overline{LN} \quad (21)$$

The associated FS firing forte is

$$\underline{f}^s = \min(\mu_{\underline{US}}(Var, a), \mu_{\underline{US}}(dVar, a)) \quad (22)$$

$$\overline{f}^s = \max(\mu_{\overline{US}}(Var, a), \mu_{\overline{US}}(dVar, a)) \quad (23)$$

$$F^S = [\underline{f}^s, \overline{f}^s] \quad (24)$$

TR is used to convert T2 FS to type-1 FS. The techniques used for defuzzification is center of sets (SOC). The results are as follows:

$$Y_{\cos} = \sum_{s=1}^{25} \frac{F^s Y^s}{F^s} = [Y_{m1}, Y_{m2}] \quad (25)$$

$$Y_{m1} = \frac{\sum_{s=1}^{25} \underline{f}^s Y^s}{\sum_{s=1}^{25} \underline{f}^s} \quad (26)$$

$$Y_{m2} = \frac{\sum_{s=1}^{25} \overline{f}^s Y^s}{\sum_{s=1}^{25} \overline{f}^s} \quad (27)$$

where Y_{m1} and Y_{m2} are linked to 2 MF of type-1 FLC. The output is obtained by averaging.

4. OPTIMIZATION PROBLEM

In the existing effort, an integral squared-based objective function (J) to reduce the frequency deviation and control action is formulated as cost function J :

Set the no. of particles (n), maximum no. of iteration (Max_I_t), Dimension, lower/upper bounds of variables & the algorithm parameters
 Initialize the particle's positions $i=1,2,\dots, n$
 Set the fitness of equilibrium candidates' to a high value
 while ($I_t < Max_I_t$)
 for $i=1:n$
 Find the fitness of i -th particle
 If $fit(\vec{X}_i) < fit(\vec{X}_{E1})$
 Replace \vec{X}_{E1} with \vec{X}_i
 Else if $fit(\vec{X}_i) > fit(\vec{X}_{E1}) \ \& \ fit(\vec{X}_i) < fit(\vec{X}_{E2})$
 Replace \vec{X}_{E2} with \vec{X}_i
 Else if $fit(\vec{X}_i) > fit(\vec{X}_{E1}) \ \& \ fit(\vec{X}_i) > fit(\vec{X}_{E2}) \ \& \ fit(\vec{X}_i) < fit(\vec{X}_{E3})$
 Replace \vec{X}_{E3} with \vec{X}_i
 Else if $fit(\vec{X}_i) > fit(\vec{X}_{E1}) \ \& \ fit(\vec{X}_i) > fit(\vec{X}_{E2}) \ \& \ fit(\vec{X}_i) > fit(\vec{X}_{E3}) \ \& \ fit(\vec{X}_i) < fit(\vec{X}_{E4})$
 Replace \vec{X}_{E4} with \vec{X}_i
 End (if)
 End (for)
 Calculate \vec{X}_{EAv} using Eq. (43)
 Form the equilibrium pool using Eq. (32)
 Carry out memory saving (if $I_t > 1$)
 Set 't' using Eq. (34)
 for $i=1:n$
 Randomly select one candidate from the equilibrium pool
 Generate random vectors of \vec{r}_1 & $\vec{\alpha}$ & construct \vec{E}_i using Eq. (36)
 Generate \vec{G}_{rc} , \vec{G}_{r0} & \vec{G}_r using Eqs. (39)-(37)
 Update \vec{X} using Eq. (40)
 End (for)
 $I_t = I_t + 1$
 End (while)

FIGURE 4. Pseudo code for SCAIEO algorithm.

$$J = \int_0^t \left[k_n w \left\{ \sum (\Delta f_i)^2 + (\Delta P_{Tie})^2 \right\} + (1-w) \left\{ \sum (\Delta U_i)^2 \right\} \right] dt \quad (28)$$

where t is the time, Δf_i and ΔP_{Tie} are the frequency deviation of area- i & tieline power, and ΔU_i controller output of area- i . To make certain that all the terms in Eq. (19) contribute in optimization process, the weighting factors k_n and w are allocated values of 1000 and 0.5 correspondingly.

Now, the problem is characterized by:

$$\text{Minimize } J \quad (29)$$

$$\text{Subject to } K_{P_i \min} \leq K_{P_i} \leq K_{P_i \max}, K_{I_i \min} \leq K_{I_i} \leq K_{I_i \max}, \\ K_{1 \min} \leq K_1 \leq K_{1 \max}, K_{2 \min} \leq K_2 \leq K_{2 \max} \quad (30)$$

The limiting parameters are represented by the subscripts "min/max."

Method	Parameter	Explanation
PSO	Social & cognitive components, c_1 & c_2	2
	Inertia weight, w	Reduces from 0.9 to 0.2
DA	Inertia weight, w	Reduces s from 0.9 to 0.2
	Alignment & Separation weight, s & a	0.1
ABC	Food factor f , Cohesion, c , and Enemy position, e	0.7, 1,1
	% of onlooker bees & employed bees	50% of the colony
MFO	Scout bees	1
	Convergence constant, r	Reduces from -1 to -2
GSA	Value of G_o and Constant, α	1, 20
PSOGSA	Social & Cognitive components, c_1 & c_2	2
	Value of G_o and Constant, α	1, 20
CS	Step size, α and Number of nests, n	1, 15
	Probability of discovering Cuckoo's egg by the host bird, p_x	0.25
WCA	Total no. of rivers, N_{sr}	8
	Search intensity near the sea, d_{max}	1 E - 03
	Factor μ	0.1
WCMFO	Convergence factor, a	Reduces from -1 to -2
	Total no. of rivers, N_{sr}	8
	Search intensity near the sea, d_{max}	1 E - 03
GA	Crossover rate and mutation rate	0.9 and 0.2
	Selection	Tournament
EO	Algorithm parameters	$c_1=2, c_2=1, G_p=0.5$
	Equilibrium pool vector	$\vec{X}_{E,PL} = (\vec{X}_{E1}, \vec{X}_{E2}, \vec{X}_{E3}, \vec{X}_{E4}, \vec{X}_{EAv})$
	Average position calculation	$\vec{X}_{EAv} = \frac{(\vec{X}_{E1} + \vec{X}_{E2} + \vec{X}_{E3} + \vec{X}_{E4})}{4}$
SCaIEO	Algorithm parameters	$c_1=2, c_2=1, G_p=0.5$
	Equilibrium pool vector	$\vec{X}_{E,PL} = (\vec{X}_{E1}, \vec{X}_{E2}, \vec{X}_{E3}, \vec{X}_{EAv})$
	Average position calculation	$\vec{X}_{EAv} = \frac{\text{SCaSF}(5\vec{X}_{E1} + 3\vec{X}_{E2} + 2\vec{X}_{E3})}{10 * \text{SCaSF}}$
	Scaling factor ($W=100$)	$\begin{cases} W * \sin\left(\frac{I_t}{\text{Max}I_t}\right) \text{ if } \text{RND1} < 0.5 \\ W * \cos\left(\frac{I_t}{\text{Max}I_t}\right) \text{ if } \text{RND1} \geq 0.5 \end{cases}$

TABLE 3. Parameter of various methods.

5. SINE COSINE ADOPTED IMPROVED EQUILIBRIUM OPTIMIZATION (SCAIEO) ALGORITHM

EO is a new optimization technique motivated by control volume mass equilibrium models engaged to assessment of various states.

The overviews of some terms/steps of EO are:

5.1. Initialization

The initial population is created as per the problem dimension as:

$$X_i^{\text{Int}} = X_{\min} + \text{RND}_i(X_{MX} - X_{MN}), \quad i = 1, 2, \dots, n \quad (31)$$

X_i^{Int} is the initial vector of the i th particle, X_{MN} and X_{MX} are limiting values for the dimensions, RND_i is a arbitrary vector in the range $[0,1]$, and n is the no. of particles.

5.2. Equilibrium Pool and Candidates (X_E)

Five particles are engaged to build an equilibrium pool as:

$$\vec{X}_{E,PL} = (\vec{X}_{E1}, \vec{X}_{E2}, \vec{X}_{E3}, \vec{X}_{E4}, \vec{X}_{EAv}) \quad (32)$$

5.3. Exponential Term (E_t)

An exponential term (E_t) is used in updating rule and is calculated as:

Function	IEO		EO		GA [43]		PSO [43]	
	Avg.	Std.Dev	Avg.	Std.Dev	Avg.	Std.Dev	Avg.	Std.Dev
$bf_1(y)$	0	0	1.58 E - 202	0	8 E - 4	8.7 E - 4	7.38 E - 54	2.17 E - 53
$bf_2(y)$	0	0	1.35 E - 110	4.73 E - 110	3 E - 3	1.8 E - 3	5.68 E - 31	1.38 E - 30
$bf_3(y)$	0	0	9.34 E - 113	2.64 E - 112	13.213	8.042	3.15 E - 18	9.67 E - 18
$bf_4(y)$	0	0	4.71 E - 77	1.72 E - 77	0.209	5.8 E - 2	4.3E - 16	9.76E - 16
$bf_5(y)$	3.3411	0.2315	3.181	0.1669	16.913	22.375	3.311	1.647
$bf_6(y)$	5.14 E - 34	2.31 E - 33	0	0	7.5 E - 4	7.2 E - 4	0	0
$bf_7(y)$	3.37 E - 05	2.94 E - 05	8.51 E - 05	5.47 E - 05	8.1 E - 4	5.5 E - 4	1.4 E - 3	7 E - 4
Function	DA [43]		WCA [43]		GSA [43]		MFO [43]	
	Avg.	Std.Dev	Avg.	Std.Dev	Avg.	Std.Dev	Avg.	Std.Dev
$bf_1(y)$	5.303 E - 1	1.3180	3.1E - 14	5.8E - 14	1.02 E - 18	3.3 E - 19	1.65 E - 31	4.91 E - 31
$bf_2(y)$	2.392	3.912	2.11 E - 07	3.96 E - 07	2.33 E - 09	4.39 E - 10	2.69 E - 19	6.22 E - 19
$bf_3(y)$	215.45	935.17	3.56 E - 12	9.56 E - 12	1.00 E - 05	5.50 E - 05	2.05 E - 11	4.21 E - 11
$bf_4(y)$	1.153	2.702	1.08 E - 11	5.73 E - 11	4.76 E - 10	8.44 E - 11	5.79 E - 06	3.17 E - 05
$bf_5(y)$	6784.5	21974.5	1.252	1.831	5.423	0.1238	133.11	555.57
$bf_6(y)$	2.2023	5.528	4.6 E - 18	2.26 E - 17	6.40 E - 19	2.30 E - 19	4.78 E - 32	1.27 E - 31
$bf_7(y)$	6.9 E - 3	7.6 E - 3	0.5155	0.2552	1.86 E - 3	6.7 E - 4	1.2 E - 3	7.2 E - 4
Function	CS [43]		PSOGSA [43]		ABC [43]		WCMFO [43]	
	Avg.	Std.Dev	Avg.	Std.Dev	Avg.	Std.Dev	Avg.	Std.Dev
$bf_1(y)$	9.48E - 13	1.46E - 2	1.24 E - 20	3 E - 21	1.93E - 2	1.46E - 2	1.10 E - 95	6.05E - 95
$bf_2(y)$	1.67 E - 05	1.3 E - 2	2.58 E - 10	4.57 E - 11	3.42 E - 2	1.3 E - 2	3.52 E - 33	1.35 E - 32
$bf_3(y)$	2.17 E - 06	227.45	2.48 E - 20	9.34 E - 21	848.34	227.45	1.62 E - 32	8.88 E - 32
$bf_4(y)$	4.9 E - 03	1.938	6.35 E - 11	1.26 E - 11	7.939	1.938	3.29E - 24	1.31E - 23
$bf_5(y)$	0.68946	0.57142	1.1607	2.0941	44.513	15.196	2.4259	3.467
$bf_6(y)$	1.48 E - 12	8.3 E - 13	1.38 E - 20	3.37 E - 21	1.13 E - 2	7.3 E - 3	6.97 E - 29	3.29 E - 28
$bf_7(y)$	4.735 E - 3	1.754 E - 3	2.3 E - 3	1.2 E - 3	3.93 E - 2	1.09 E - 2	0.4987	0.305

TABLE 4. (a) Results for 10-dimensional unimodal benchmark functions.

Function	IEO		EO		GA [43]		PSO [43]	
	Av.	St.Dev	Av.	St.Dev	Av.	St.Dev	Av.	St.Dev
$bf_8(y)$	-3321.2	242.6	-3318.2	247.2	-3692.39	182.42	-2742.78	274.7175
$bf_9(y)$	0	0	0	0	3.8 E - 4	3.2 E - 4	1.757	1.1592
$bf_{10}(y)$	8.88 E - 16	0	3.49 E - 15	1.59 E - 15	8.88 E - 16	1.0 E - 31	8.88 E - 16	1.00 E - 31
$bf_{11}(y)$	0	0	0	0	5.6 E - 2	3 E - 2	0.1244	8.04E - 2
$bf_{12}(y)$	4.71 E - 32	1.9 E - 34	4.71 E - 32	1.8 E - 34	5.73 E - 05	1.4 E - 4	4.71 E - 32	1.67 E - 47
$bf_{13}(y)$	1.35 E - 32	2.3 E - 34	1.35 E - 32	0	6.21 E - 05	1.1 E - 4	1.34 E - 32	5.56 E - 48
Function	DA [43]		WCA [43]		GSA [43]		MFO [43]	
	Av.	St.Dev	Av.	St.Dev	Av.	St.Dev	Av.	St.Dev
$bf_8(y)$	-3213.66	431.748	-3422.55	304.572	-1694.53	190.6721	-3329.13	288.317
$bf_9(y)$	11.561	10.177	20.993	10.524	1.392	1.214	12.8372	7.352
$bf_{10}(y)$	3.14 E - 05	1.7 E - 04	2.42 E - 15	1.79 E - 15	1.28 E - 10	6.71 E - 11	8.88 E - 16	1.00 E - 31
$bf_{11}(y)$	0.3846	0.3826	0.1502	9.44 E - 2	1.67 E - 2	2.79 E - 2	1.78 E - 01	8.43 E - 02
$bf_{12}(y)$	0.5296	0.6912	1.036 E - 2	5.67 E - 2	7.95 E - 21	3.23 E - 21	3.11 E - 02	9.487 E - 2
$bf_{13}(y)$	0.5292	0.7173	7.3 E - 4	2.7 E - 3	5.67 E - 20	1.88 E - 20	1.10 E - 3	3.33 E - 3
Function	CS [43]		PSOGSA [43]		ABC [43]		WCMFO [43]	
	Av.	St.Dev	Av.	St.Dev	Av.	St.Dev	Av.	St.Dev
$bf_8(y)$	-3712.01	167.4447	-3271.6	278.08	-3922.73	88.61857	-3729.7	96.325
$bf_9(y)$	6.574	1.367	23.281	12.968	3.677	1.0365	2.089	1.508
$bf_{10}(y)$	1.24 E - 15	1.08 E - 15	4.94 E - 12	2.26 E - 12	1.21 E - 06	9.37 E - 07	8.88 E - 16	1.00 E - 31
$bf_{11}(y)$	3.96 E - 02	8.8 E - 3	0.2004	0.1141	0.281	0.1086	9.91 E - 02	5.31 E - 2
$bf_{12}(y)$	9.77 E - 05	1.3 E - 4	0.2491	0.581	1.9 E - 3	1.3 E - 3	2.00 E - 29	6.44 E - 29
$bf_{13}(y)$	1.31 E - 09	1.39 E - 09	3.11 E - 21	1.06 E - 21	8.3 E - 3	5.1 E - 3	4.49 E - 22	2.06 E - 21

TABLE 4. (b) Results for 10-dimensional multi-modal benchmark function.

Function	IEO		EO		GA [43]		PSO [43]	
	Av.	St.Dev	Av.	St.Dev	Av.	St.Dev	Av.	St.Dev
$bf_{14}(y)$	0.998	0	0.998	0	0.998	8.83 E - 14	1.56	0.959
$bf_{15}(y)$	3.0 E - 4	7.6 E - 6	1 E - 3	3.7 E - 3	8.4 E - 4	2.9 E - 4	7 E - 4	3.2 E - 4
$bf_{16}(y)$	-1.0316	0	-1.0316	0	-1.03	5.02 E - 10	-1.03	3
$bf_{17}(y)$	3.98 E - 1	0	3.98 E - 1	0	3.98 E - 1	4.73 E - 7	3.98 E - 1	1.13 E - 16
$bf_{18}(y)$	3	0	3	0	3	1.21 E - 8	3	4.52 E - 16
$bf_{19}(y)$	-3.86	2.64 E - 15	-3.86	2.67 E - 15	-3.86	2.203 E - 3	-3.86	2.7 E - 15
$bf_{20}(y)$	-3.25	6.01 E - 2	-3.25	6.03 E - 2	-3.32	2.170 E - 2	-3.26	6.04 E - 2
Function	DA [43]		WCA [43]		GSA [43]		MFO [43]	
	Av.	St.Dev	Av.	St.Dev	Av.	St.Dev	Av.	St.Dev
$bf_{14}(y)$	1.1	0.303	0.998	3.39 E - 16	3.4	2.578637	1.03	0.1814836
$bf_{15}(y)$	1.34 E - 3	5.11 E - 4	3.69 E - 4	2.32 E - 4	1.8 E - 3	4.9 E - 4	8.37 E - 4	2.54 E - 4
$bf_{16}(y)$	-1.03	2.55 E - 11	-1.03	0	-1.03	0	-1.03	0
$bf_{17}(y)$	3.98 E - 1	7.6 E - 13	3.98 E - 1	3.79 E - 16	3.98 E - 1	1.13 E - 16	3.98 E - 1	1.13 E - 16
$bf_{18}(y)$	3	1.38 E - 6	3	1.79 E - 14	3	4.02 E - 15	3	1.95 E - 15
$bf_{19}(y)$	-3.86	1.587 E - 03	-3.86	2.71 E - 15	-3.86	2.71 E - 15	-3.86	2.71 E - 15
$bf_{20}(y)$	-3.25	6.72 E - 02	-3.26	6.04 E - 2	-3.32	1.36 E - 15	-3.22	4.5066 E - 2
Function	CS [43]		PSO GSA [43]		ABC [43]		WCMFO [43]	
	Av.	St.Dev	Av.	St.Dev	Av.	St.Dev	Av.	St.Dev
$bf_{14}(y)$	0.998	3.39 E - 16	1.06	0.252	0.998	1.02E - 13	0.998	5.36 E - 16
$bf_{15}(y)$	3 E - 4	4.23 E - 9	3.79 E - 3	7.5 E - 3	7 E - 4	1.3 E - 4	3.0 E - 4	1.07 E - 15
$bf_{16}(y)$	-1.03	0	-1.03	0	-1.03	7.36 E - 11	-1.03	0
$bf_{17}(y)$	3.98 E - 1	1.13 E - 16	3.98 E - 1	1.13 E - 16	3.98 E - 1	5.68 E - 09	3.98 E - 1	1.13 E - 16
$bf_{18}(y)$	3	4.52 E - 16	3	4.52 E - 16	3	8.64 E - 05	3	9.57 E - 15
$bf_{19}(y)$	-3.86	2.71 E - 15	-3.86	2.71 E - 15	-3.86	7.89 E - 11	-3.86	2.71 E - 15
$bf_{20}(y)$	-3.32	1.26 E - 13	-3.26	6.032 E - 2	-3.32	4.82 E - 06	-3.25	6.027 E - 2

TABLE 4. (c) Results for fixed-dimensional multi-modal benchmark function.

Technique/Controller	Controller-1			Controller-2			J value
	K_P	K_I	K_D	K_P	K_I	K_D	
GA/PID	1.5860	1.1862	1.2653	0.0269	0.3272	0.0201	9.9342
PSO/PID	1.4998	1.4903	1.4839	0.0165	0.0019	0.0021	8.4844
MFO/PID	1.6878	1.6771	1.6699	0.0018	0.0019	1.6412	6.9061
GSA/PID	1.7277	1.7166	1.7093	0.0018	0.0019	1.6799	6.6421
EO/PID	1.8029	1.7914	1.7837	0.1557	1.7731	1.7530	6.4883
SCaIEO/PID	1.8979	1.8779	1.8979	0.0018	0.0019	1.8779	5.6855

TABLE 5. Optimal parameters for PID controller.

$$\vec{E}_t = e^{-\alpha(t-t_0)} \quad (33)$$

where time, t , is a function of iteration (It) given by:

$$t = \left(1 - \frac{I_t}{\text{Max}_I_t}\right)^{\left(c_1 \frac{I_t}{\text{Max}_I_t}\right)} \quad (34)$$

where I_t and Max_I_t are the present and the maximum number of iterations, and c_1 is a constant which manages exploitation capability. The parameter t_0 is calculated as:

$$\vec{t}_0 = \frac{1}{\alpha} \ln [-c_2 \text{sign}(\vec{r}_1 - 0.5) (1 - e^{-\vec{\alpha}t})] + t \quad (35)$$

where c_2 is a constant which manages the exploration capability, and r_1 is a value from 0 and 1.

So \vec{E}_t can be stated as:

$$\vec{E}_t = c_2 \text{sign}(\vec{r}_1 - 0.5) (e^{-\vec{\alpha}t} - 1) \quad (36)$$

5.4. Generation Rate (G_r)

The G_r helps in improving the exploitation phase of EO and calculated as:

$$\vec{G}_r = \vec{G}_{r0}^{-\alpha(t-t_0)} = \vec{G}_{r0}\vec{E}_t \quad (37)$$

where

$$\vec{G}_{r0} = \vec{G}_{rc}(\vec{X}_E - \vec{\alpha}\vec{X}) \quad (38)$$

$$\vec{G}_{rc} = \begin{cases} 0.5r_2 & \text{if } r_3 \geq G_p \\ 0 & \text{if } r_3 < G_p \end{cases} \quad (39)$$

where r_2 and r_3 are random values in $[0, 1]$, G_{rc} is Generation rate Control factor, and G_p is Generation Probability.

The updating rule of EO is:

$$\vec{X} = \vec{X}_E + (\vec{X} - \vec{X}_E) \cdot \vec{E}_t + \left(\frac{G_r}{\alpha C_V} - \vec{E}_t \right) \quad (40)$$

Where C_V is control volume.

In the proposed optimization technique, four best elements beside the average of element are employed to shape the

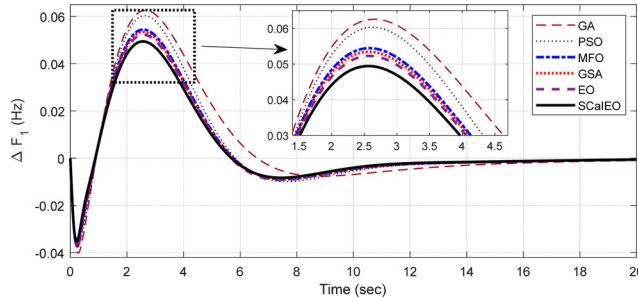


FIGURE 5. Comparison of techniques.

equilibrium pool vector as Eq. (32). The average of particles is found by in Eq. (41). In the suggested SCaIEO method, the equilibrium pool vector is constructed by considering only three best-so-far particles as given in Eq. (42). Also, in original EO, equal importance is given to all particles irrespective of their fitness as given in Eq. (41), where as in proposed SCaIEO, more weightage is given to the best particles as given in Eq. (43)

$$\vec{X}_{EA_V} = \frac{(\vec{X}_{E1} + \vec{X}_{E2} + \vec{X}_{E3} + \vec{X}_{E4})}{4} \quad (41)$$

$$\vec{X}_{E,PL} = (\vec{X}_{E1}, \vec{X}_{E2}, \vec{X}_{E3}, \vec{X}_{EA_V}) \quad (42)$$

$$\vec{X}_{EA_V} = \frac{\text{SCaSF}(\vec{5X}_{E1} + \vec{3X}_{E2} + \vec{2X}_{E3})}{10 * \text{SCaSF}} \quad (43)$$

SCaSF is the sine cosine adapted scaling factor (SF):

$$\text{ScaSF} = \begin{cases} W * \sin\left(\frac{I_t}{\text{Max}_I_t}\right) & \text{if } \text{RND1} < 0.5 \\ W * \cos\left(\frac{I_t}{\text{Max}_I_t}\right) & \text{if } \text{RND1} \geq 0.5 \end{cases} \quad (44)$$

RND1 is a random quantity in the limit $[0, 1]$, and W is a weighting factor. The optimal solution sites are unknown in the early stages. As a result, taking large steps initially may have an influence on particles distant from the ideal placements. As a result, SF are used to vary the effort of

Controller/ Technique	Integral errors				Max. overshoots (MO _s)			Max. undershoots (MU _s) (-ve)	
	ISE × 10 ⁻²	ITAE	ITSE × 10 ⁻²	IAE × 10 ⁻¹	ISTAE	ΔF ₁ × 10 ⁻²	ΔF ₂ × 10 ⁻²	ΔF ₁ × 10 ⁻²	ΔF ₂ × 10 ⁻²
GA/PID	1.9561	2.8556	6.2655	5.6664	26.1249	6.2561	5.9394	4.0211	2.7024
PSO/PID	1.6678	2.4301	5.1681	5.0817	20.8221	6.0309	5.6918	3.7616	2.5105
MFO/PID	1.3509	2.1535	4.1012	4.5567	18.3866	5.4437	5.1163	3.7321	2.4473
GSA/PID	1.2981	2.1048	3.9304	4.4625	17.9491	5.3425	5.0174	3.6922	2.4179
EO/PID	1.2411	2.0466	3.7721	4.3652	17.1578	5.2267	4.9068	3.6265	2.3678
SCaIEO/PID	1.1063	1.9318	3.3342	4.1139	16.4018	4.9427	4.6312	3.5238	2.2908

TABLE 6. Comparison of Performance index for different techniques.

Technique/Controller	Controller area-1					Controller area-2					J value
	K _I	K ₂	K _P	K _I	K _D	K _I	K ₂	K _P	K _I	K _D	
T1FPID	1.9255	1.7845	1.8241	1.6826	1.2532	0.3007	1.8779	0.1070	0.0017	0.0307	1.6778
T2FPID	1.1679	1.2731	1.7957	1.7209	0.3463	0.3007	0.1591	0.1829	0.0017	0.0018	0.7862
AT2FPID	1.8779	1.8070	1.8979	1.8979	1.8054	1.5001	0.0305	1.8961	0.1707	1.5975	0.2188
			1.8679	1.8731	0.3852			1.8979	1.8721	0.0402	

TABLE 7. Tuned controller parameters for SCaIEO.

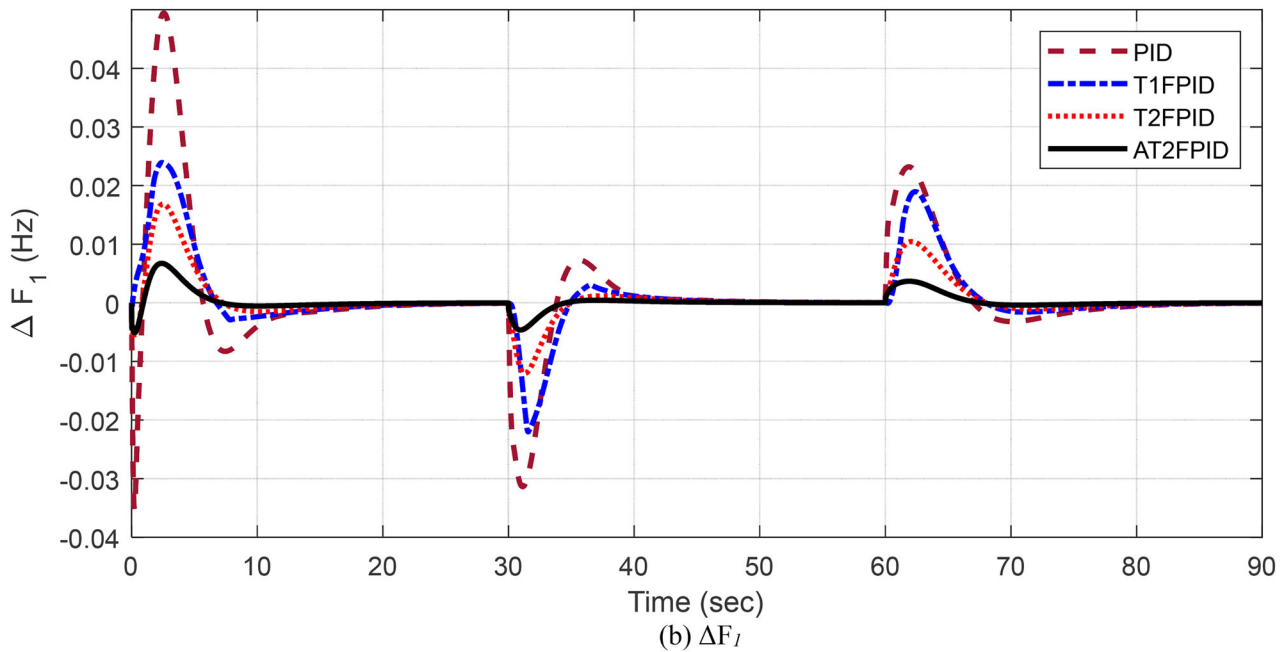
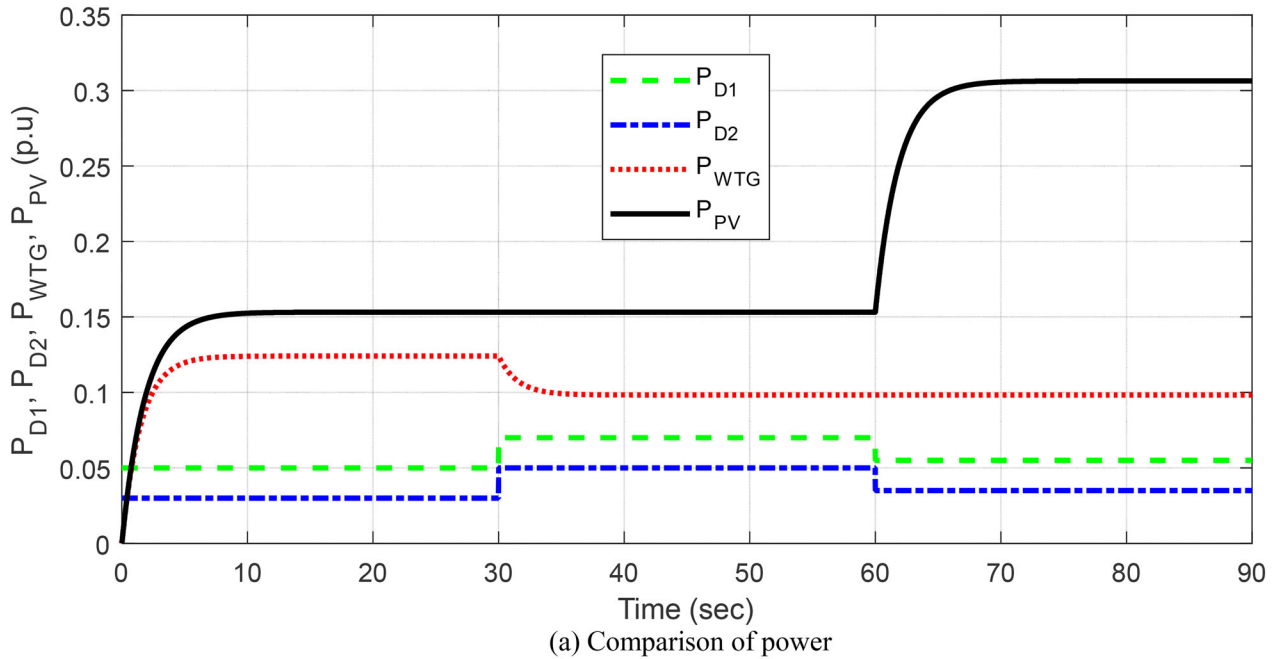


FIGURE 6. Responses for Case 1 (a) Comparison of power (b) ΔF_1 (c) ΔF_2 .

particles in the premature phases of the process. For proper selection of weights, several values for W are attempted and assessed. It has been discovered that best results are obtained at W is set to 100. The pseudocodes of the proposed optimization algorithm is provided in Figure 4.

6. RESULTS AND DISCUSSION

6.1. Authentication of SCAIEO

In this work, the recommended SCAIEO is verified on several standard benchmark functions (*bf's*) as given in Ref.

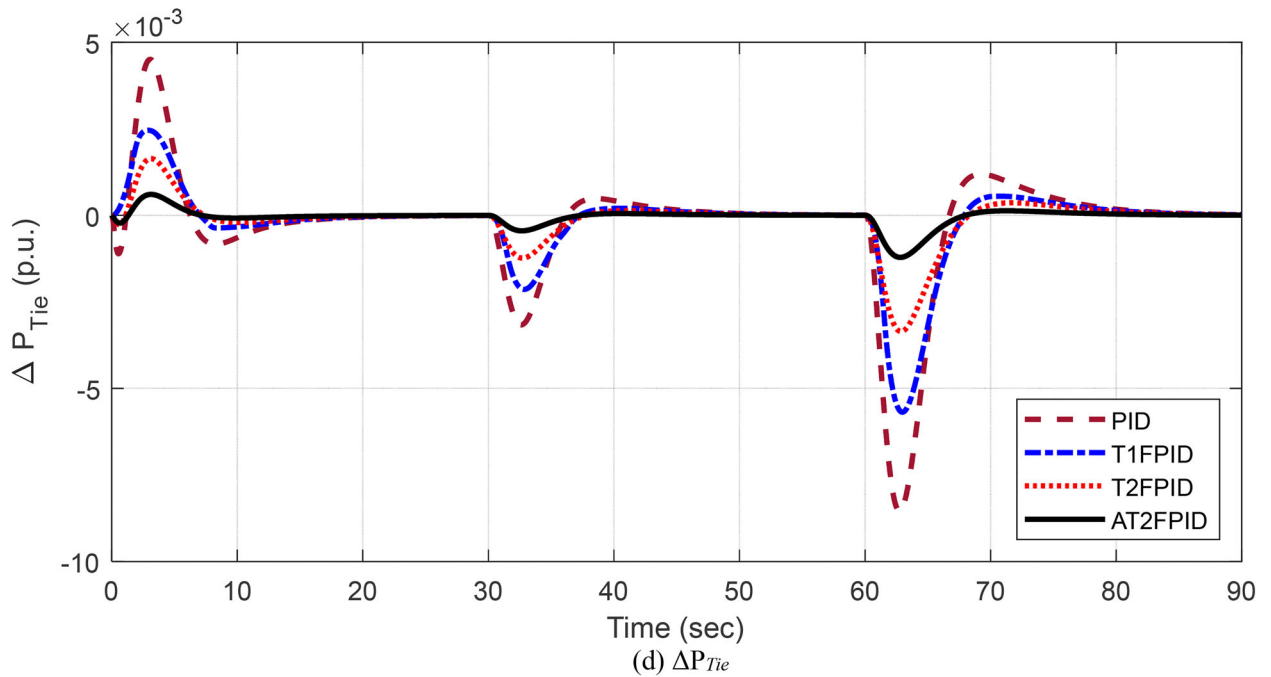
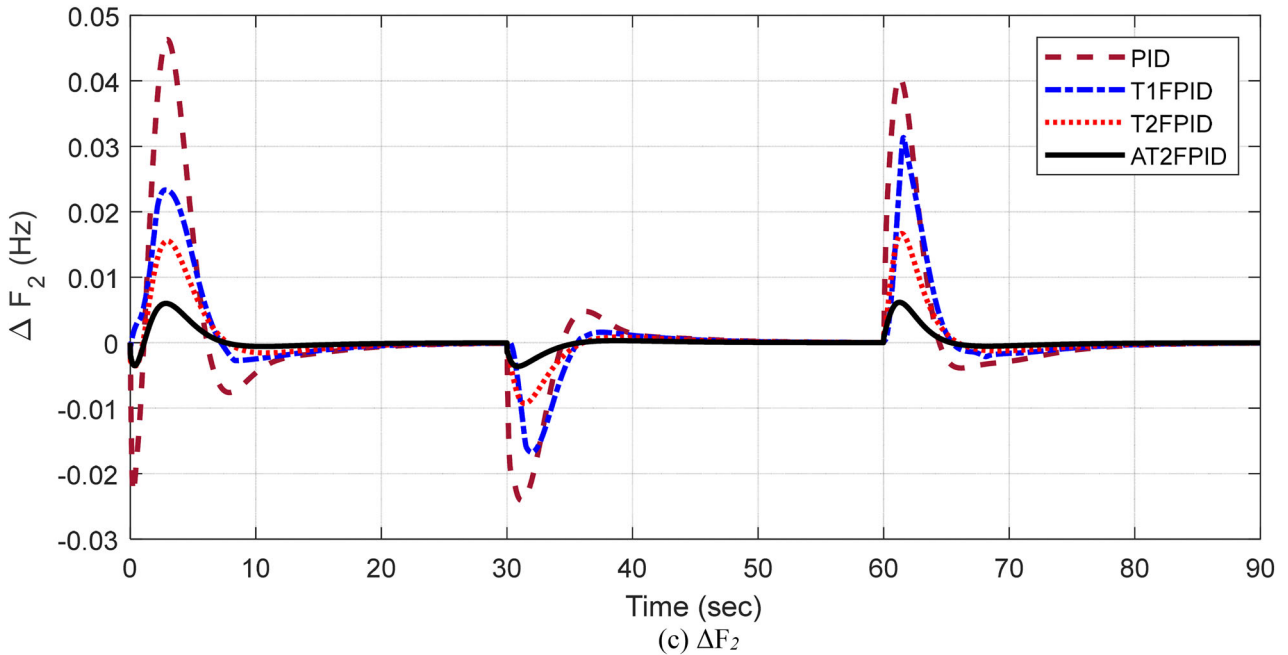


FIGURE 6. Continued.

[34]. Functions 1 to 7 are 10-dimensional unimodal *bf*'s, 8 to 13 are 10-dimensional multi-modal *bf*'s and 14 to 20 are multi-modal *bf*'s of fixed dimensions. To validate the worth of the proposed SCAIEO technique, it is compared to EO and various recently developed optimization processes such as [34–43] as presented in Ref. [43]. For all techniques,

the number of function evaluations is set at 100,000 to ensure fair assessment. One thousand iterations with hundred number of search agents are considered in the anticipated SCAIEO. The parameters of all procedures are taken from the literature [14–21, 31] and compiled in Table 3. Tables 4(a)–4(c) show the average and standard deviation

Controller/ Technique	J value	Errors					(MO _s)		(MU _s)	
		ISE $\times 10^{-3}$	ITAE	ITSE $\times 10^{-2}$	IAE $\times 10^{-1}$	ISTAE $\times 10^2$	ΔF_1 $\times 10^{-2}$	ΔF_2 $\times 10^{-2}$	ΔF_1 $\times 10^{-2}$	ΔF_2 $\times 10^{-2}$
PID	10.1729	19.4397	27.8935	45.2447	9.1472	14.8231	2.3185	4.0397	0.3212	0.3872
T1FPID	3.91047	7.1264	18.6332	21.7302	5.5965	10.0862	1.8951	3.1343	0.1577	0.2129
T2FPID	1.72046	2.1748	11.9025	7.7211	3.5923	6.4841	1.0431	1.6663	0.1048	0.1252
AT2FPID	0.55453	0.4086	4.3142	1.0561	1.3567	2.3406	0.3674	0.6169	0.0401	0.0528

TABLE 8. Comparative results for Case 1.

values of the objective function obtained in 30 runs for 10-dimensional unimodal bf's, 10-dimensional multi-modal bf's, and fixed-dimensional unimodal bf's, respectively. For comparison, the results of Ref. [43] are also gathered in Tables 4(a)–4(c) from which it can be seen that suggested SCAIEO outperforms other considered techniques in 11 out of 13 bf's of 10-dimension. For remaining 7 bf's of fixed dimension, SCAIEO provides equally best results in all 7 bf's.

6.2. Implementation of SCAIEO for Controller Design

The efficacy of the recommended approach for LFC of the examined PS revealed in Figure 1 is evaluated. Table 1 displays the system data. A five percent disturbance in area 1 and a three percent SLP in area 2 are used to calculate the goal function. The system frequency changes due to load disturbances. The frequency fluctuation is controlled by the proper execution of controllers. To validate the superiority of the SCAIEO approach, a PID controller is used initially, and the gains are determined using the SCAIEO, EO, GSA, MFO, PSO, and GA methods. The controller parameter range has been set to [0, 2]. For each method, 30 search agents and 100 iterations are chosen. All techniques are performed 30 times, and the best results achieved as the lowest J value supplied by Eq. (19) in 30 runs are employed as the final settings. Table 5 shows the results, which show that EO ($J=6.4883$) has a lower J value than GA ($J=9.9342$), PSO ($J=8.4844$), MFO ($J=6.9061$), and GSA ($J=6.6421$). When SCAIEO is on, the J value drops to 5.6855. The percentage decrease in J value using the SCAIEO approach for GA, PSO, MFO, GSA, and EO is 42.76%, 32.98%, 17.67%, 14.4%, and 12.37%, accordingly. Figure 5 depicts the ΔF_1 response to the aforementioned disruption. As shown in Figure 4, the performance of the SCAIEO approach with the PID structure outperforms the GA, PSO, MFO, GSA, and EO procedures.

Table 6 illustrates the assessment of transient characteristics ΔF_1 , ΔF_2 , ΔP_{Tie} of the proposed system with PID controller adjusted by the preceding methodologies employing multiple parameters. It is witnessed that the mathematical values integral errors (ISE = 1.1063×10^{-2} , ITAE = 1.9318, ITSE = 3.3342×10^{-2} , IAE = 4.1139×10^{-1} , ISTAE = 16.4018), maximum overshoots ($O_s = 4.9427 \times 10^{-2}$ and 4.6312×10^{-2}) and maximum undershoots ($U_s = 3.5238 \times 10^{-2}$ and 2.2908×10^{-2}) due to SCAIEO enhanced PID controller is shown to be the least when compared to GA, PSO, MFO, GSA, and EO optimized PID controller. This validates the SCAIEO technique's superiority over GA, PSO, MFO, GSA, and EO methodologies in the controller design issue.

In the next step, similar previous generation PID and Adaptive Type-2 Fuzzy PID (AT2FPID) structures are optimized by SCAIEO method. The results are gathered in Table 7. It is apparent that, less J worth is achieved with AT2FPID ($J=0.2188$) compared to T2FPID ($J=0.7862$) and T1FPID ($J=1.6778$).

The following instances are being reviewed further:

- Case 1: Change in SLPs with the variation in wind speed and sun irradiance.
- Case 2: The effect of a 100% increase in wind and solar power on SLPs.
- Case 3: Increasing SLPs due to a lack of wind and Photovoltaic electricity
- Case 4: Uncertainty in system parameter
- Case 5: Inclusion of physical constraints

Case 1:

In this case, change in SLPs, wind speed and sun irradiance is considered. Figure 5(a) depicts these load and power changes (a). Figures 6(b)–6(d) show the response with SCAIEO-based PID, T1FPID, T2FPID, and AT2FPID (d). Table 8 shows the numerical values of different integral errors the studied system. It is noted that the numerical values J ($J=0.2899$), errors (ISE = 0.2256×10^{-3} , ITAE = 0.7331, ITSE = 0.0929×10^{-2} , IAE = 0.7219×10^{-1} , ISTAE = 18.421), MUs (0.1752×10^{-2} , 0.1162×10^{-2}) and MUs

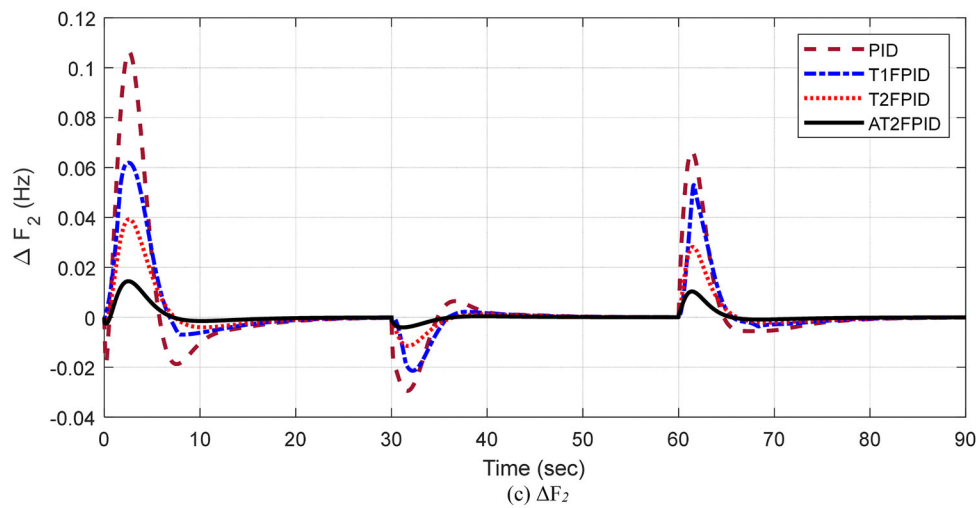
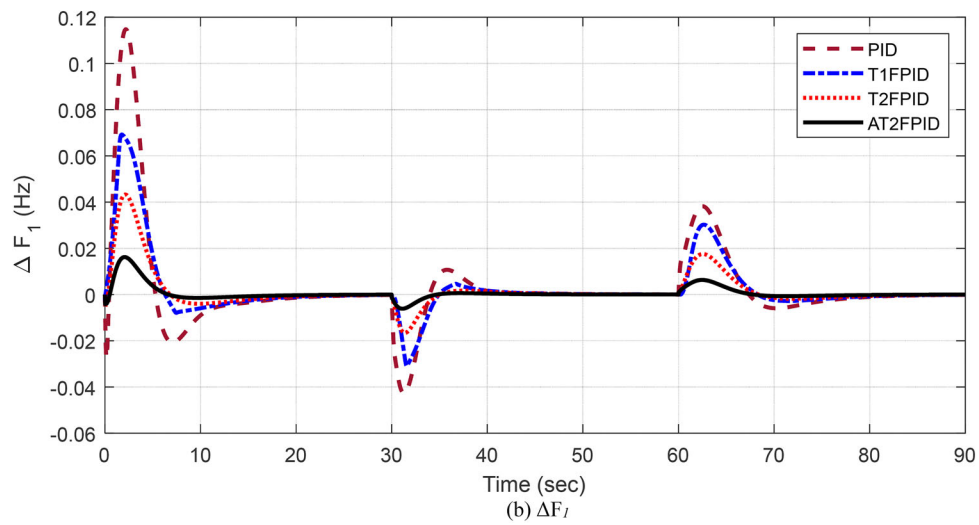
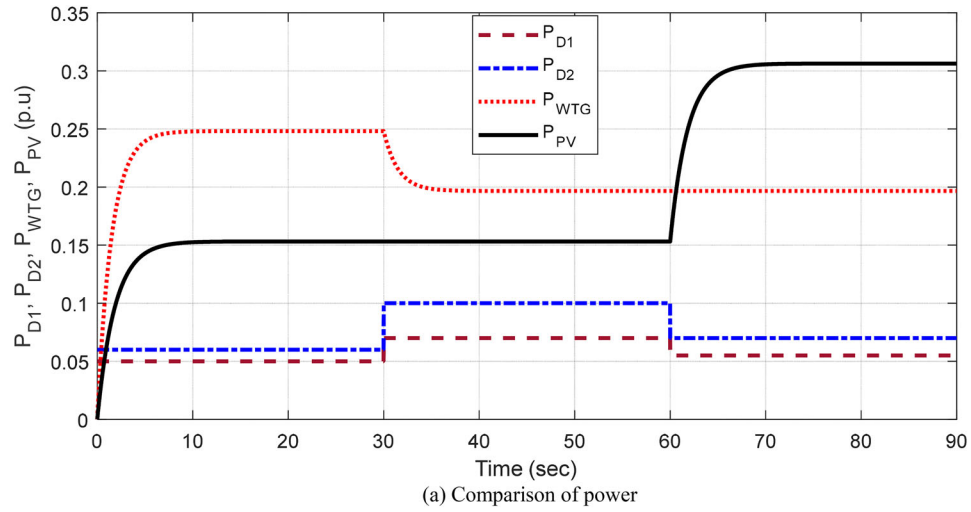


FIGURE 7. Responses for Case 2 (a) Comparison of power (b) ΔF_1 (c) ΔF_2 .

Controller/ Technique	J value	Errors					(MO _s)		(MU _s)	
		ISE $\times 10^{-3}$	ITAE	ITSE $\times 10^{-1}$	IAE $\times 10^{-1}$	ISTAE $\times 10$	ΔF_1 $\times 10^{-2}$	ΔF_2 $\times 10^{-2}$	ΔF_1 $\times 10^{-2}$	ΔF_2 $\times 10^{-2}$
PID	41.6738	77.4027	47.713	12.4756	17.3786	25.4611	11.4779	10.6277	4.2684	2.9468
T1FPID	18.3791	32.6743	32.0967	6.1477	11.3064	17.3292	6.9232	6.1924	3.0951	2.1415
T2FPID	8.2598	12.4296	20.7899	2.2738	7.2006	11.3109	4.3294	3.9318	1.6579	1.1495
AT2FPID	2.8948	1.6489	7.4621	0.3012	2.5947	4.0544	1.6213	1.4461	0.6135	0.4041

TABLE 9. Comparative results for Case 2.

(0.16335×10^{-2} , 0.1085) owing to SCAIEO optimized AT2FPID controller are determined to be least compared to other techniques. In Case 1, the AT2FPID approach reduces J value by 67.76%, 85.81%, and 94.54% when compared to T2FPID, T1FPID, and PID controllers, respectively.

Case 2:

In this case, wind and solar power are enhanced by 100%. Figure 6(a) depicts these power fluctuations (a). Figures 7(b) and 7(c) show the reaction with SCAIEO-based PID, T1FPID, T2FPID, and AT2FPID. In comparison to other structures, the response of the SCAIEO-based AT2FPID regulator is better. Table 9 shows the arithmetical values of different errors for investigated Case. As compared to alternative techniques, the numerical values of J , integral errors, and Mos/MUs owing to the SCAIEO optimized AT2FPID controller are determined to be the lowest. The percentage reduction of J value using AT2FPID approach compared to previous generation controller is 64.95%, 84.24%, and 93.05% in Case 2.

Case 3:

Wind and solar power are no longer accessible, whereas SLP-1 and SLP-2 are boosted by 200% and 100%, respectively, relative to nominal SLPs as indicated in Case 1. Figure 8(a) depicts these power fluctuations. Figures 7(b) and 7(c) show the response with SCAIEO-based PID, T1FPID, T2FPID, and AT2FPID. In comparison to other controllers, the transient performance of the SCAIEO-based AT2FPID controller is greater. Table 10 displays the arithmetical values of different performance for Case 3. As compared to alternative techniques, the J , errors, and Mos/MUs caused by the SCAIEO optimized AT2FPID controller are determined to be the lowest. In Case 3, the AT2FPID approach reduces J value by 62.59%, 81.87%, and 93.2% when compared to T2FPID, T1FPID, and PID controllers, respectively.

Case 4:

In actual systems, the parameters used to build the system are likely to be imprecise. Moreover, the settings may vary over time, influencing system performance. As a

result, it is critical to analyze system performance under system parameter fluctuations. In this scenario, uncertainties in system parameters are examined to assess the adaptability and resilience of the projected control approach. The following situations are being consideration:

Scenario 1: The system R , T_g , T_t , B and loading are increased by 25%

Scenario 2: The system R , T_g , T_t , B and loading are decreased by 25%

Scenario 3: The system R , T_g , T_t , B and loading are varied randomly by -25%, 50%, 75%, -20% and 100%, respectively.

Numerical values of various parameters, of frequency responses, ΔP_{Tie} of the investigated system with SCAIEO optimized AT2FPID controller for Case 4 is given in Table 11. For better illustration, the percentage deviations for each scenario are also provided in Table 11. As an example, the ΔF_1 for the above scenarios are revealed in Figure 9. It is obvious from Figure 9 and Table 11 that SCAIEO optimized AT2FPID controller performs satisfactorily in existence of parameter uncertainty.

Case 5:

To get an accurate comprehension of the AGC issues, it is obligatory to take account of the vital intrinsic non-linearities that are present in power system. The major non-linearities are Governor Dead Band (GBD and Generation Rate Constraint (GRC) [5]. Therefore, this work is further stretched by including a GRC of 3%/min and GBD of 0.036 Hz in system model [5]. To examine the consequence of physical constraints, the optimum parameters which were obtained without considering non-linearities mentions in Case 1 are considered.

The results with SCAIEO-based PID, T1FPID, T2FPID, and AT2FPID are exhibited in Figure 10. It can be seen that, the performance degrades when non-linearities are considered. But, the response with SCAIEO optimized AT2FPID controller is greater in contrast to other controllers. The comparative results for Case 5 are specified in Table 12 which confirms the improved performance of

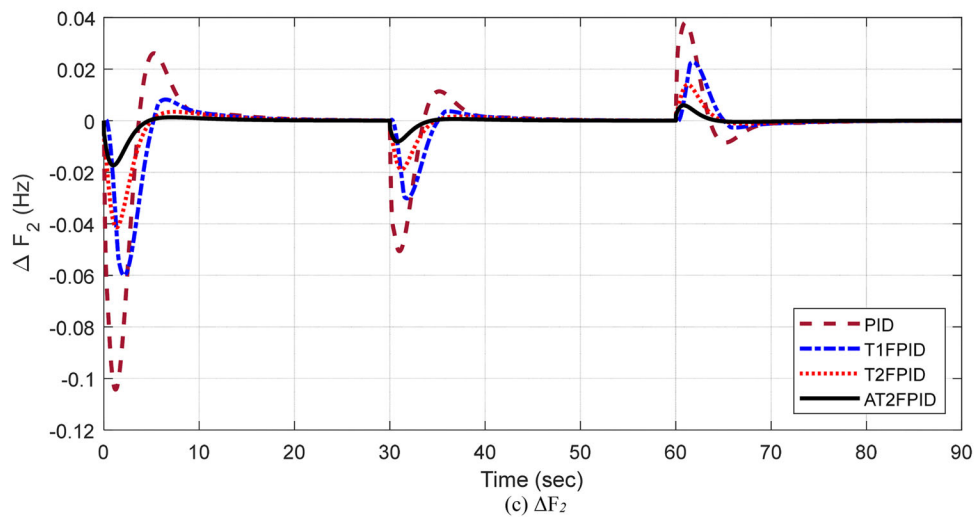
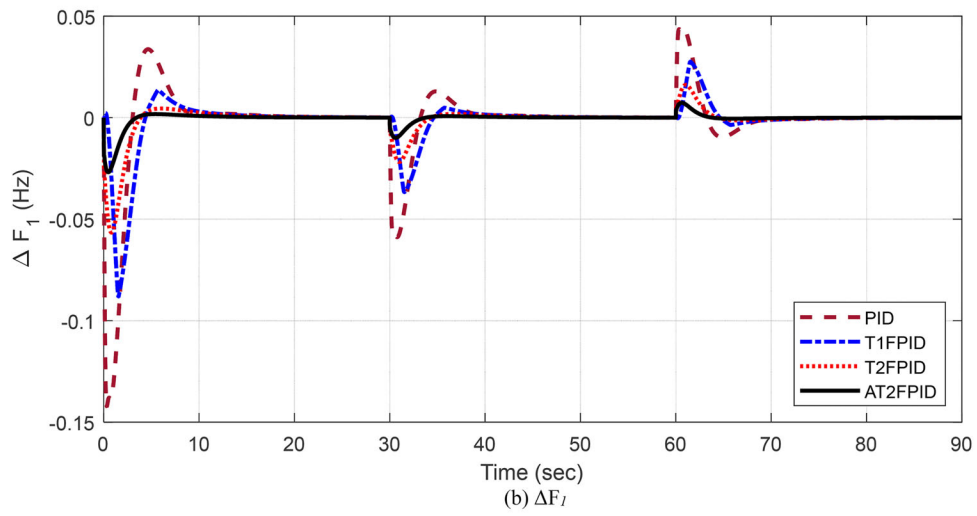
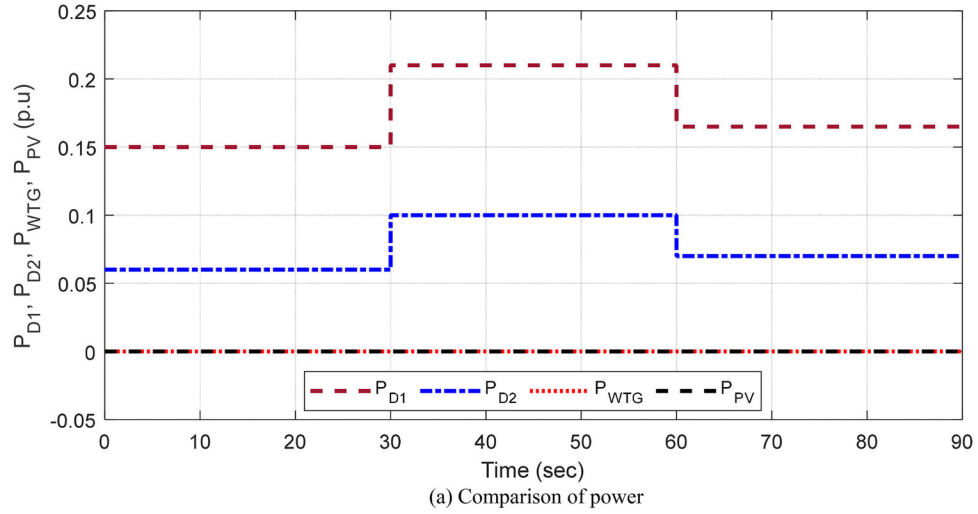


FIGURE 8. Responses for Case 3.

Controller/ Technique	J value	Errors				(MO _s)		(MU _s)		
		ISE $\times 10^{-3}$	ITAE	ITSE $\times 10^{-1}$	IAE $\times 10^{-1}$	ISTAE $\times 10$	ΔF_1 $\times 10^{-2}$	ΔF_2 $\times 10^{-2}$	ΔF_1 $\times 10^{-2}$	ΔF_2 $\times 10^{-2}$
PID	36.7124	69.4853	30.1216	7.8151	13.8274	14.3092	4.4245	3.8051	14.2256	10.4318
T1FPID	13.7588	24.3991	18.4592	2.9725	8.2071	8.7489	2.7564	2.2657	8.8148	6.0028
T2FPID	6.6685	10.2161	11.2281	1.0336	5.2085	5.3444	1.6097	1.3979	5.6614	4.1438
AT2FPID	2.4941	1.8086	4.2794	0.1721	2.0358	2.03388	0.7315	0.5961	2.6902	1.7343

TABLE 10. Comparative results for Case 3.

Controller/ Technique	J value $\times 10^{-2}$	Errors				(MO _s)		(MU _s)		
		ISE $\times 10^{-3}$	ITAE	ITSE $\times 10^{-2}$	IAE $\times 10^{-1}$	ISTAE $\times 10^2$	ΔF_1 $\times 10^{-2}$	ΔF_2 $\times 10^{-2}$	ΔF_1 $\times 10^{-3}$	ΔF_2 $\times 10^{-3}$
Nominal	55.4534	0.4086	4.3143	1.0561	1.3567	2.3406	0.6723	0.6169	0.5106	0.3621
Scenario 1 (S1)	49.2389	0.2829	3.6025	0.7311	1.1281	1.9598	0.5653	0.5305	0.5411	0.3391
% variation for S1	-11.21	-30.76	-16.49	-30.77	-16.84	-16.26	-15.91	-14.01	5.97	-6.35
Scenario 2 (S2)	68.4109	0.6684	5.4953	1.7283	1.7326	2.9742	0.8412	0.7922	0.5722	0.4604
% variation for S2	23.36	63.58	27.37	63.64	27.71	27.07	25.12	28.41	12.06	27.14
Scenario 3(S3)	70.1051	0.6989	5.2101	1.7207	1.6854	2.8141	0.8816	0.8246	0.9756	0.5951
% variation for S3	26.42	71.04	20.76	62.92	24.22	20.22	31.13	33.66	91.06	64.34

TABLE 11. Comparative results for Case 4.

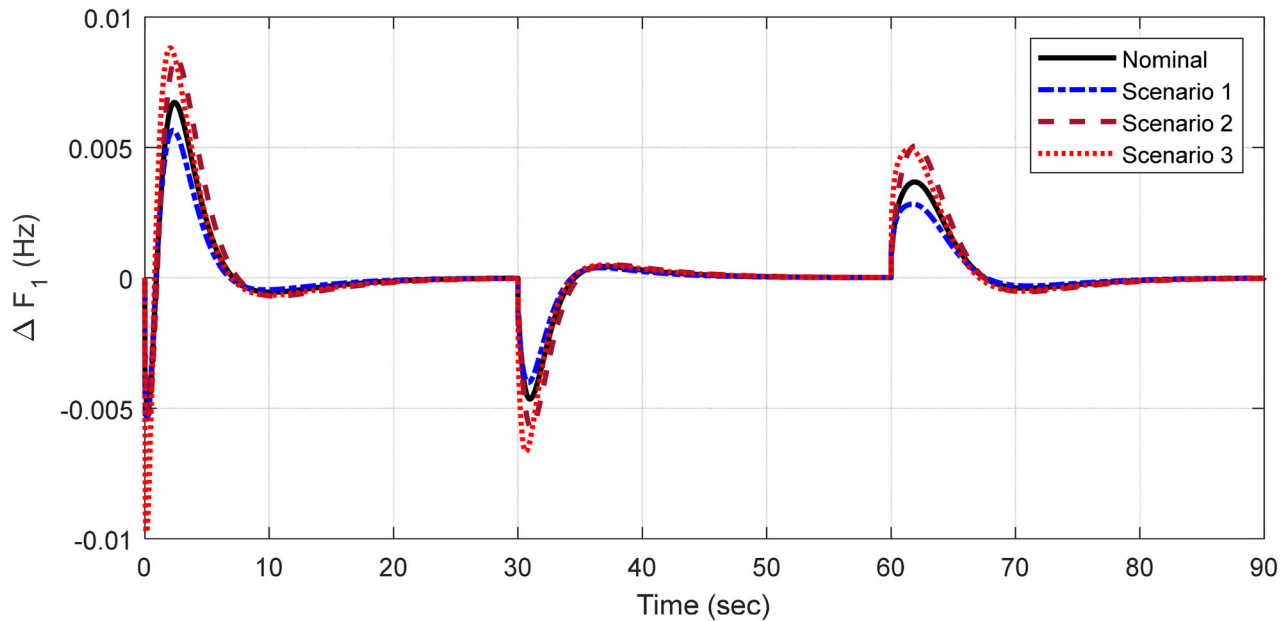
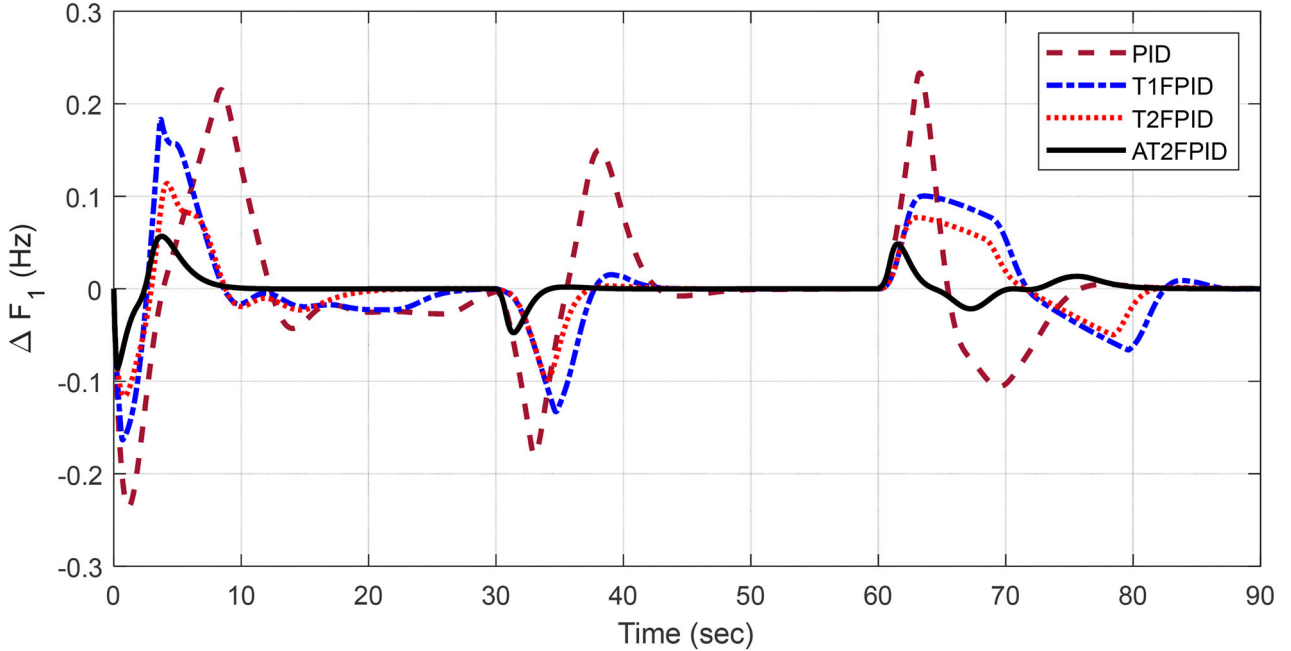


FIGURE 9. ΔF_1 response for Case 4.

Controller/Technique	J value	Errors					(MO _s)		(MU _s)	
		$ISE \times 10^{-2}$	ITAE	ITSE	IAE	$ISTAE \times 10^3$	ΔF_1	ΔF_2	ΔF_1	ΔF_2
PID	452.207	87.706	223.152	22.202	7.271	11.733	0.258	0.179	0.219	0.216
T1FPID	208.031	40.323	70.889	5.809	3.479	2.646	0.193	0.028	0.161	0.152
T2FPID	90.768	16.873	39.486	2.024	2.199	1.426	0.155	0.156	0.102	0.106
AT2FPID	23.942	3.672	4.467	0.811	0.128	0.2669	0.056	0.063	0.085	0.053

TABLE 12. Comparative results for Case 5.


 FIGURE 10. ΔF_1 responses for Case 5.

AT2FPID r . When non-linearities are considered, the % decrease in J value with AT2FPID compared to T2FPID, T1FPID, and PID regulators are 73.62%, 88.49%, and 94.71, respectively.

7. CONCLUSION

To resolve optimization and engineering problems, a Sine Cosine Adopted Improved Equilibrium Optimization (SCaIEO) approach was suggested in this research. Taking benchmark functions demonstrates the SCaIEO's supremacy over EO and other optimization techniques. The methodology is then used to create AT2FPID controllers with a % reduction in J value using the SCaIEO method for GA, PSO, MFO, GSA, and EO of 42.76%, 32.98%, 17.67%, 14.4%, and 12.37%, respectively. Moreover, for the identical step load perturbations in each region, the % reduction in J value

with AT2FPID related to T2FPID, T1FPID, and PID is 72.16%, 86.95%, and 96.15%, respectively. When all disturbances are evaluated (Case 3), the AT2FPID approach reduces J value by 67.76%, 85.81%, and 94.54% when compared to T2FPID, T1FPID, and PID controllers, respectively. It is also observed that the suggested AT2FPID technique handles non-linearity better than existing approaches. When non-linearities are taken into account, the percentage reduction in J value using AT2FPID approach compared to previous generation PID controllers are 73.62%, 88.49%, and 94.71. The current analysis is applicable to a big system with multiple systems.

Keeping in view of recent trends, Electric Vehicles (EV) may be included in the system model and FLC scheme for EVs to contribute in the LFC of MGs may be studied. Also, owing to the low inertia of microgrids, virtual inertia control concept may be explored for better frequency regulation.

CONFLICT OF INTEREST

We declare that there is no conflict of interest.

ORCID

Sanjeevikumar Padmanaban  <http://orcid.org/0000-0003-3212-2750>

REFERENCES

- [1] O. I. Elgerd, *Electric Energy Systems Theory*. New Delhi: Tata McGraw Hill, 2006.
- [2] R. K. Khadanga, A. Kumar, and S. Panda, "A novel modified whale optimization algorithm for load frequency controller design of a two-area power system composing of PV grid and thermal generator," *Neural Comput. Appl.*, vol. 32, no. 12, pp. 8205–8216, 2020. DOI: [10.1007/s00521-019-04321-7](https://doi.org/10.1007/s00521-019-04321-7).
- [3] B. Mohanty, S. Panda, and P. K. Hotta, "Controller parameters tuning of differential evolution algorithm and its application to load frequency control of multisource power system," *Int. J. Electr. Power Energy Syst.*, vol. 54, pp. 77–85, 2014. DOI: [10.1016/j.ijepes.2013.06.029](https://doi.org/10.1016/j.ijepes.2013.06.029).
- [4] R. K. Sahu, S. Panda, and S. Padhan, "Optimal gravitational search algorithm for interconnected power systems," *Ain Shams Eng. J.*, vol. 5, no. 3, pp. 721–733, 2014. DOI: [10.1016/j.asej.2014.02.004](https://doi.org/10.1016/j.asej.2014.02.004).
- [5] S. Panda, B. Mohanty, and P. K. Hota, "Hybrid BFOA-PSO algorithm for automatic generation control of linear and nonlinear interconnected power systems," *Appl. Soft Comput.*, vol. 13, no. 12, pp. 4718–4730, 2013. DOI: [10.1016/j.asoc.2013.07.021](https://doi.org/10.1016/j.asoc.2013.07.021).
- [6] R. K. Sahu, S. Panda, and G. T. C. Sekhar, "A novel hybrid PSO-PS optimized fuzzy PI controller for AGC in multi area interconnected power systems," *Int. J. Electr. Power Energy Syst.*, vol. 64, pp. 880–893, 2015.
- [7] Y. Arya, "Improvement in automatic generation control of two-area electric power systems via a fuzzy aided optimal PIDN-FOI controller," *ISA Trans.*, vol. 80, pp. 475–490, 2018.
- [8] Y. Arya and N. Kumar, "BFOA-scaled fractional order fuzzy PID controller applied to AGC of multi-area multi-source electric power generating systems," *Swarm Evol. Comput.*, vol. 32, pp. 202–218, 2017.
- [9] P. C. Sahu, S. Mishra, R. C. Prusty, and S. Panda, "Improved-salp swarm optimized type-II fuzzy controller in load frequency control of multi area islanded AC microgrid," *Sustain. Energy, Grids Netw.*, vol. 16, pp. 380–392, 2018.
- [10] A. Fereidouni, A. S. Masoum, and M. Moghbel, "A new adaptive configuration of PID type fuzzy logic controller," *ISA Trans.*, vol. 56, pp. 222–240, 2015.
- [11] S. Padhy and S. Panda, "Application of a simplified Grey Wolf optimization technique for adaptive fuzzy PID controller design for frequency regulation of a distributed power generation system," *Prot. Control Mod. Power Syst.*, vol. 6, no. 1, pp. 1–16, 2021. DOI: [10.1186/s41601-021-00180-4](https://doi.org/10.1186/s41601-021-00180-4).
- [12] S. K. Bhatta, S. Mohapatra, P. C. Sahu, S. C. Swain, and S. Panda, "Load frequency control of a diverse energy source integrated hybrid power system with a novel hybridized harmony search-random search algorithm designed Fuzzy-3D controller," *Energy Sources A: Recovery Util. Environ. Effects*, pp. 1–22, 2021. DOI: [10.1080/15567036.2021.1970860](https://doi.org/10.1080/15567036.2021.1970860).
- [13] P. C. Sahu, R. C. Prusty, and S. Panda, "Active power management in wind/solar farm integrated hybrid power system with AI based 3DOF-FOPID approach," *Energy Sources A: Recovery, Util. Environ. Effects*, pp. 1–21, 2021. DOI: [10.1080/15567036.2021.1956647](https://doi.org/10.1080/15567036.2021.1956647).
- [14] P. C. Pradhan, R. K. Sahu, and S. Panda, "Comparative performance analysis of hybrid differential evolution and pattern search technique for frequency control of the electric power system," *J. Electr. Syst. Inform. Technol.*, vol. 8, pp. 1–21, 2021.
- [15] D. Mohanty, R. K. Sahu, P. C. Pradhan, and S. Panda, "Design and analysis of the 2DOF-PIDN-FOID controller for frequency regulation of the electric power systems," *Int. J. Ambient Energy*, pp. 1–14, 2021. DOI: [10.1080/01430750.2021.1909134](https://doi.org/10.1080/01430750.2021.1909134).
- [16] P. C. Nayak, R. C. Prusty, and S. Panda, "Grasshopper optimization algorithm optimized multistage controller for automatic generation control of a power system with FACTS devices," *Prot. Control Mod. Power Syst.*, vol. 6, no. 1, pp. 15, 2021. DOI: [10.1186/s41601-021-00187-x](https://doi.org/10.1186/s41601-021-00187-x).
- [17] P. C. Nayak, B. P. Nayak, R. C. Prusty, and S. Panda, "Sunflower optimization based fractional order fuzzy PID controller for frequency regulation of solar-wind integrated power system with hydrogen aqua equalizer-fuel cell unit," *Energy Sources A: Recovery Util. Environ. Effects*, pp. 1–19, 2021. DOI: [10.1080/15567036.2021.1953636](https://doi.org/10.1080/15567036.2021.1953636).
- [18] S. Mishra, R. C. Prusty, and S. Panda, "Performance analysis of modified sine cosine optimized multistage FOPDPI controller for load frequency control of an islanded microgrid system," *Int. J. Numer. Model.*, vol. 34, no. 6, pp. 1–26, 2021. DOI: [10.1002/jnm.2923](https://doi.org/10.1002/jnm.2923).
- [19] P. C. Nayak, A. Sahoo, R. Balabantaray, and R. C. Prusty, "Comparative study of SOS & PSO for fuzzy based PID controller in AGC in an integrated power system," *IEEE Conf. Technol. Smart – City Energy Security Power*, vol. 1, pp. 1–6, 2018.
- [20] R. K. Khadanga, A. Kumar, and S. Panda, "Frequency control in hybrid distributed power systems via type-2 fuzzy PID controller," *IET Renew. Power Gen.*, vol. 15, no. 8, pp. 1706–1723, 2021. DOI: [10.1049/rpg2.12140](https://doi.org/10.1049/rpg2.12140).
- [21] R. K. Khadanga, A. Kumar, and S. Panda, "Application of interval type-2 fuzzy PID controller for frequency regulation of AC islanded microgrid using modified equilibrium optimization algorithm," *Arab. J. Sci. Eng.*, vol. 46, no. 10, pp. 9831–9847, 2021. DOI: [10.1007/s13369-021-05580-0](https://doi.org/10.1007/s13369-021-05580-0).
- [22] M. Elsis and M. Soliman, "Optimal design of robust resilient automatic voltage regulators," *ISA Trans.*, vol. 108, pp. 257–268, 2021. DOI: [10.1016/j.isatra.2020.09.003](https://doi.org/10.1016/j.isatra.2020.09.003).
- [23] M. M. Ismail, A. F. Bendary, and M. Elsis, "Optimal design of battery charge management controller for hybrid

- system PV/wind cell with storage battery,” *IJPEC.*, vol. 11, no. 4, pp. 412–429, 2020. DOI: [10.1504/IJPEC.2020.110018](https://doi.org/10.1504/IJPEC.2020.110018).
- [24] M. A. E. Mohamed *et al.*, “Optimal energy management solutions using artificial intelligence techniques for photovoltaic empowered water desalination plants under cost function uncertainties,” *IEEE Access*, vol. 10, pp. 93646–93658, 2022. DOI: [10.1109/ACCESS.2022.3203692](https://doi.org/10.1109/ACCESS.2022.3203692).
- [25] M. Elsis, “Design of neural network predictive controller based on imperialist competitive algorithm for automatic voltage regulator,” *Neural Comput. Appl.*, vol. 31, no. 9, pp. 5017–5027, 2019. DOI: [10.1007/s00521-018-03995-9](https://doi.org/10.1007/s00521-018-03995-9).
- [26] R. K. Khadanga *et al.*, “A novel optimal robust design method for frequency regulation of three-area hybrid power system utilizing Honey Badger algorithm,” *Int. Trans. Electr. Energy Syst.*, vol. 2022, pp. 1–11, 2022. DOI: [10.1155/2022/6017066](https://doi.org/10.1155/2022/6017066).
- [27] S. Mishra, P. C. Nayak, R. C. Prusty, and S. Panda, “Modified multiverse optimizer technique-based two degree of freedom fuzzy PID controller for frequency control of microgrid systems with hydrogen aqua electrolyzer fuel cell unit,” *Neural Comput. Appl.*, vol. 34, no. 21, pp. 18805–18821, 2022. DOI: [10.1007/s00521-022-07453-5](https://doi.org/10.1007/s00521-022-07453-5).
- [28] S. Padhy *et al.*, “Marine predator algorithm based PD-(1+PI) controller for frequency regulation in multi-microgrid system,” *IET Renew. Power Gen.*, vol. 16, no. 10, pp. 2136–2151, 2022. DOI: [10.1049/rpg2.12504](https://doi.org/10.1049/rpg2.12504).
- [29] A. Kumar, R. K. Khadanga, and S. Panda, “Reinforced modified equilibrium optimization technique-based MS-PID frequency regulator for a hybrid power system with renewable energy sources,” *Soft Comput.*, vol. 26, no. 11, pp. 5437–5455, 2022. DOI: [10.1007/s00500-021-06558-8](https://doi.org/10.1007/s00500-021-06558-8).
- [30] A. Alorf, “A survey of recently developed metaheuristics and their comparative analysis,” *Eng. Appl. Artif. Intell.*, vol. 117, pp. 105622, 2023. DOI: [10.1016/j.engappai.2022.105622](https://doi.org/10.1016/j.engappai.2022.105622).
- [31] A. Faramarzi, M. Heidarnejad, B. Stephens, and S. Mirjalili, “Equilibrium optimizer: A novel optimization algorithm,” *Knowl. Based Syst.*, vol. 191, pp. 105190, 2020. DOI: [10.1016/j.knsys.2019.105190](https://doi.org/10.1016/j.knsys.2019.105190).
- [32] B. Zhou, K. W. Chan, T. Yu, and C. Y. Chung, “Equilibrium-inspired multiple group search optimization with synergistic learning for multiobjective electric power dispatch,” *IEEE Trans. Power Syst.*, vol. 28, no. 4, pp. 3534–3545, 2013. DOI: [10.1109/TPWRS.2013.2259641](https://doi.org/10.1109/TPWRS.2013.2259641).
- [33] X. Zhang *et al.*, “Equilibrium-inspired multiagent optimizer with extreme transfer learning for decentralized optimal carbon-energy combined-flow of large-scale power systems,” *Appl. Energy*, vol. 189, pp. 157–176, 2017. DOI: [10.1016/j.apenergy.2016.12.080](https://doi.org/10.1016/j.apenergy.2016.12.080).
- [34] D. Karaboga and B. Basturk, “A powerful and efficient algorithm for numerical function optimization: Artificial bee colony (ABC) algorithm,” *J. Glob. Optim.*, vol. 39, no. 3, pp. 459–471, 2007. DOI: [10.1007/s10898-007-9149-x](https://doi.org/10.1007/s10898-007-9149-x).
- [35] J. H. Holland, “Genetic algorithms,” *Sci. Am.*, vol. 267, no. 1, pp. 66–72, 1992. DOI: [10.1038/scientificamerican0792-66](https://doi.org/10.1038/scientificamerican0792-66).
- [36] X. S. Yang and S. Deb, “Cuckoo search via Lévy flights,” presented at the 2009 World Congress on Nature & Biologically Inspired Computing, IEEE, Coimbatore, India, 2009.
- [37] J. Kennedy and R. Eberhart, “Particle swarm optimization,” presented at the Proceedings of the IEEE International Conference on Neural Networks, Perth, WA, Australia, 1995, pp. 1942–1948.
- [38] E. Rashedi, H. Nezamabadi-Pour, and S. Saryazdi, “GSA: A gravitational search algorithm,” *Inf. Sci.*, vol. 179, no. 13, pp. 2232–2248, 2009. DOI: [10.1016/j.ins.2009.03.004](https://doi.org/10.1016/j.ins.2009.03.004).
- [39] S. Mirjalili and S. Z. M. Hashim, “A new hybrid PSO-GSA algorithm for function optimization,” presented at the Computer and Information Application (ICCIA), Tianjin, China, IEEE, 2010, pp. 374–377.
- [40] H. Eskandar, A. Sadollah, A. Bahreinejad, and M. Hamdi, “Water cycle algorithm—A novel metaheuristic optimization method for solving constrained engineering optimization problems,” *Comput. Struct.*, vol. 110–111, pp. 151–166, 2012. DOI: [10.1016/j.compstruc.2012.07.010](https://doi.org/10.1016/j.compstruc.2012.07.010).
- [41] S. Mirjalili, “Moth-flame optimization algorithm: A novel nature inspired heuristic paradigm,” *Knowl. Based Syst.*, vol. 89, pp. 228–249, 2015. DOI: [10.1016/j.knsys.2015.07.006](https://doi.org/10.1016/j.knsys.2015.07.006).
- [42] S. Mirjalili, “Dragonfly algorithm: A new meta-heuristic optimization technique for solving single-objective, discrete and multi-objective problems,” *Neural Comput. Appl.*, vol. 27, no. 4, pp. 1053–1073, 2016. DOI: [10.1007/s00521-015-1920-1](https://doi.org/10.1007/s00521-015-1920-1).
- [43] S. Khalilpourazari and S. Khalilpourazary, “An efficient hybrid algorithm based on water cycle and moth-flame optimization algorithms for solving numerical and constrained engineering optimization problems,” *Soft Comput.*, vol. 23, no. 5, pp. 1699–1722, 2019. DOI: [10.1007/s00500-017-2894-y](https://doi.org/10.1007/s00500-017-2894-y).
- [44] D. L. Lee and L. Wang, “Small-signal stability analysis of an autonomous hybrid renewable energy power generation/energy storage system part I: Time-domain simulations,” *IEEE Trans. Energy Convers.*, vol. 23, no. 1, pp. 311–320, 2008. DOI: [10.1109/TEC.2007.914309](https://doi.org/10.1109/TEC.2007.914309).
- [45] K. Singh, M. Amir, F. Ahmad, and M. A. Khan, “An integral tilt derivative control strategy for frequency control in multi-microgrid system,” *IEEE Syst. J.*, vol. 15, no. 1, pp. 1477–1488, 2021. DOI: [10.1109/JSYST.2020.2991634](https://doi.org/10.1109/JSYST.2020.2991634).

BIOGRAPHIES

Srinivasan Kullapadayachi Govindaraju is currently working as Assistant Professor in the Department of Electrical and Electronics Engineering in Mahendra Engineering College for Women has teaching experience of Eight Years and research experience of Five years. He has completed his Bachelor and Master’s Degree from Anna University in the year 2012 and 2014, respectively. He has completed Doctoral degree in the Faculty of Electrical Engineering from Anna University Chennai in the year 2022. He is Expert in the field of renewable energy and smart grid technologies and act as Recognized

reviewer for various reputed journal. He has Published two research papers in international peer reviewed journals.

Raghuraman Sivalingam is an expert in the field of Power systems and renewable energy technologies has teaching experience of 22 years and currently working as Assistant Professor in Department of Electrical and Electronics Engineering of Velammal Engineering College Chennai, Tamilnadu. He has completed bachelor degree in Electrical and Electronics Engineering from Bharathiar University Coimbatore in year 2000 and completed masters in Power System Engineering from Anna University Chennai in year 2007 and completed his PhD in Faculty of Electrical Engineering at SRM University Chennai in the year 2017. He is a Recognized research supervisor in Faculty of Electrical Engineering at Anna University Chennai and Recognized reviewer for various reputed journal. He has successfully guided 2 PhD scholars and currently guiding 2 PhD scholars in his research area. He has Published five research papers in international peer reviewed journals.

Sidhartha Panda is working as a Professor in the Department of Electrical Engineering, Veer Surendrai Sai University of Technology (VSSUT), Burla, Sambalpur, Odisha, India. He received Ph.D. degree from Indian Institute of Technology (IIT), Roorkee, India, M.E. degree from Veer Surendra Sai University of Technology (VSSUT). His areas of research include Flexible AC Transmission Systems (FACTS), Power System Stability, Soft computing, Model Order Reduction, Distributed Generation and Wind Energy. Dr. Panda is a Fellow of Institution of Engineers (India).

Preeti Ranjan Sahu (Student member, IEEE) received the B.Tech degree from BPUT, Rourkela, Odisha, India in 2008 and completed the M.Tech degree from Veer Surendra Sai University of Technology (VSSUT), Burla,

India in 2011. He has completed his Ph.D. degree at VSSUT, Burla, Odisha, India in 2020. He is currently working as Assistant Professor at the Department of Electrical Engineering, NIST, Berhampur, Odisha, India. His research interests include FACTS, Power System Stability and optimization techniques. He has Published 10 research papers in international peer reviewed journals.

Sanjeevikumar Padmanaban (Member'12–Senior Member'15, IEEE) received a PhD degree in electrical engineering from the University of Bologna, Bologna, Italy 2012. He is a Full Professor in Electrical Power Engineering with the Department of Electrical Engineering, Information Technology, and Cybernetics, University of South-Eastern Norway, Norway. S. Padmanaban has authored over 750+ scientific papers and received the Best Paper cum Most Excellence Research Paper Award from IET-SEISCON'13, IET-CEAT'16, IEEE-EECSI'19, IEEE-CENCON'19, and five best paper awards from ETAEERE'16 sponsored Lecture Notes in Electrical Engineering, Springer book. He is a Fellow of the Institution of Engineers, India, the Institution of Electronics and Telecommunication Engineers, India, and the Institution of Engineering and Technology, U.K. He received a lifetime achievement award from Marquis Who's Who - USA 2017 for contributing to power electronics and renewable energy research. He is listed among the world's top 2 scientists (from 2019) by Stanford University USA. He is an Editor/Associate Editor/Editorial Board for refereed journals, in particular the IEEE SYSTEMS JOURNAL, IEEE Transaction on Industry Applications, IEEE ACCESS, *IET Power Electronics*, *IET Electronics Letters*, and *Wiley-International Transactions on Electrical Energy Systems*, Subject Editorial Board Member—*Energy Sources—Energies Journal*, MDPI, and the Subject Editor for the *IET Renewable Power Generation*, *IET Generation, Transmission and Distribution*, and *FACETS Journal* (Canada).